

**MICROSCOPIC SIMULATION OF DYNAMIC FREEWAY TRAFFIC FLOW  
CONTROL APPROACHES ON AN URBAN HIGHWAY**

**M.Sc. THESIS**

**Gökhan GÖKSU**

**Department of Civil Engineering**

**Transportation Engineering Programme**

**JUNE 2013**



**MICROSCOPIC SIMULATION OF DYNAMIC FREEWAY TRAFFIC FLOW  
CONTROL APPROACHES ON AN URBAN HIGHWAY**

**M.Sc. THESIS**

**Gökhan GÖKSU  
(501111411)**

**Department of Civil Engineering**

**Transportation Engineering Programme**

**Thesis Advisor: Assoc. Prof. Dr. Murat ERGÜN**

**JUNE 2013**



**KENT İÇİ ÇEVREYOLLARINDA  
DİNAMİK TRAFİK AKIM KONTROL YAKLAŞIMLARININ  
MİKRO ÖLÇEKLİ SİMÜLASYONU**

**YÜKSEK LİSANS TEZİ**

**Gökhan GÖKSU  
(501111411)**

**İnşaat Mühendisliği Anabilim Dalı**

**Ulaştırma Mühendisliği Programı**

**Tez Danışmanı: Doç. Dr. Murat ERGÜN**

**HAZİRAN 2013**



**Gökhan GÖKSU**, a M.Sc. student of ITU Institute of Science and Technology 501111411 successfully defended the thesis entitled “**MICROSCOPIC SIMULATION OF DYNAMIC FREEWAY TRAFFIC FLOW CONTROL APPROACHES ON AN URBAN HIGHWAY**”, which he prepared after fulfilling the requirements specified in the associated legislations, before the jury whose signatures are below.

**Thesis Advisor :**     **Assoc. Prof. Dr. Murat ERGÜN** .....  
Istanbul Technical University

**Jury Members :**     **Prof. Dr. Ergun GEDİZLIOĞLU** .....  
Istanbul Technical University

**Prof. Dr. Ahmet AKBAŞ** .....  
Yalova University

**Date of Submission :**    **03 May 2013**  
**Date of Defense :**        **07 June 2013**





## FOREWORD

I would like to express my deep appreciation and thanks to Prof. Dr. Ahmet AKBAŞ for his indispensable support on VAP and for spending his valuable time and knowledge and to my advisor Assoc. Prof. Dr. Murat ERGÜN for deciding and introducing the subject. I also want to thank Prof. Dr. Mevlüt TEYMÜR for his supervision of my undergraduate thesis and drawing a vision to Transportation Engineering.

Secondly, I want to give an acknowledgment to Res. Assist. Ali Sercan KESTEN for giving me a crucial training for academia and for his collaboration, to Res. Assist. Mustafa TANIŞ for providing me RTMS data, to Mr. Bektaş KOPAL for helping me on PTV VISSIM, to Mr. Şerif AÇAK for providing me the background drawing files for simulation, to Res. Assist. Alper AKOĞUZ for his essential string finder method, to Dr. Ali DEMİRCİ, Dr. Cihangir ÖZEMİR and Res. Assist. Pınar ADANALI for helping me in L<sup>A</sup>T<sub>E</sub>X, to Res. Assist. Yusuf YEĞİNER for helping me by formatting and to Ms. Tuğba BAHAT for aiding me on AutoCAD.

Finally, I want to show my greatfulness to my mother Semra GÖKSU and my father Mustafa GÖKSU for their infinite support. I want to thank to my uncles Bayram BORA, Kadri BORA, to my family members for their valuable motivation from my highschool days, to Mr. Akar APAY and Sürat Daktilo Employees for their help while printing the thesis. I also want to remember with respect my aunt Sevil KENANOĞLU, from whom I want to take over the flag on academia and on whose memory I want to dedicate this thesis, and my uncle Bülent BORA.

Since the VAP codes have commercial value, they are not presented in this study. However, they may be downloaded from the website provided in the curriculum vitae part of this study or may be obtained upon request via e-mail or after a personal discussion.

June 2013

Gökhan GÖKSU  
(Mathematical Engineer)



## TABLE OF CONTENTS

	<u>Page</u>
<b>FOREWORD.....</b>	<b>vii</b>
<b>TABLE OF CONTENTS.....</b>	<b>ix</b>
<b>ABBREVIATIONS .....</b>	<b>xi</b>
<b>LIST OF TABLES .....</b>	<b>xiii</b>
<b>LIST OF FIGURES .....</b>	<b>xv</b>
<b>SUMMARY .....</b>	<b>xvii</b>
<b>ÖZET .....</b>	<b>xix</b>
<b>1. INTRODUCTION .....</b>	<b>1</b>
1.1 Statement of the Problem .....	1
1.2 Objectives .....	2
1.3 Literature Overview.....	3
<b>2. TRAFFIC FLOW .....</b>	<b>5</b>
2.1 Traffic Variables.....	5
2.1.1 Density.....	6
2.1.2 Flow .....	6
2.1.3 Speed .....	6
2.2 Relationship Between the Traffic Variables: MFD .....	7
2.3 Hydraulic Model: Lighthill-Whitham-Richards (LWR) Equation.....	11
2.4 Notes on Shock Waves .....	14
2.5 Improvements on LWR Equation .....	16
<b>3. TRAFFIC CONTROL APPROACHES .....</b>	<b>19</b>
3.1 Model Predictive Control (MPC) .....	19
3.2 Traffic Control Approaches .....	20
3.2.1 Ramp metering .....	20
3.2.1.1 Local (Isolated) ramp metering control strategies .....	21
3.2.1.2 Systemwide (Coordinated) ramp metering control strategies .....	21
3.2.2 Variable speed limit .....	22
3.2.3 Lane closure and allocation .....	23
<b>4. TRAFFIC SIMULATION.....</b>	<b>25</b>
4.1 Macroscopic Simulation.....	25
4.2 Microscopic Simulation.....	26
4.3 Mesoscopic Simulation .....	29
<b>5. DYNAMIC FREEWAY TRAFFIC FLOW CONTROL APPROACHES IN MICROSCOPIC TRAFFIC SIMULATOR PTV VISSIM.....</b>	<b>31</b>
5.1 Study Field.....	31

5.2 Microscopic Simulation Environment PTV VISSIM.....	35
5.2.1 Longitudinal movement model: Wiedemann Car Following Models ....	35
5.2.2 Lateral movement model .....	36
5.2.3 Network elements.....	36
5.2.4 Calibration and verification .....	37
5.3 Dynamic Traffic Flow Control Approaches in PTV VISSIM .....	39
5.3.1 Ramp metering approach.....	42
5.3.2 Variable speed limit approach .....	46
<b>6. CONCLUSION .....</b>	<b>55</b>
<b>REFERENCES.....</b>	<b>61</b>
<b>APPENDICES.....</b>	<b>67</b>
APPENDIX A .....	69
<b>CURRICULUM VITAE.....</b>	<b>81</b>

## **ABBREVIATIONS**

<b>ITS</b>	: Intelligent Transportation Systems
<b>LOS</b>	: Level of Service
<b>EDS</b>	: Elektronik Denetleme Sistemi-Turkish for "Electronic Violation Detection System"
<b>O-2</b>	: Istanbul Outer Beltway
<b>VAP</b>	: Vehicle Actuated Programming
<b>PTV VISSIM</b>	: Planung Transport Verkehr Verkehr In Städten SIMulationsmodell-German for "Planning Transport Traffic Traffic in Cities Simulation Model"
<b>LWR</b>	: Lighthill-Whitham-Richards
<b>MFD</b>	: Macroscopic Fundamental Diagram
<b>RTMS</b>	: Remote Traffic Microwave Sensor
<b>HGV</b>	: Heavy Good Vehicle
<b>OOP</b>	: Object Oriented Programming
<b>GEH</b>	: Geoffrey Edward Havers
<b>ANOVA</b>	: Analysis of Variance
<b>ALINEA</b>	: Asservissement Lineaire d'Entree Autoroutiere-French for "Linear Utilization for Highway Entrances"
<b>VSL</b>	: Variable Speed Limit
<b>HCM</b>	: Highway Capacity Manual
<b>MPC</b>	: Model Predictive Control



## LIST OF TABLES

	<u>Page</u>
<b>Table 2.1</b> : Single-Regime Models [1]. .....	9
<b>Table 2.2</b> : Multi-Regime Models [1].....	10
<b>Table 5.1</b> : The Results of Regression Analysis.....	41
<b>Table 5.2</b> : VSL Cases Offered.....	49
<b>Table A.1</b> : Average Delay Time per Vehicle in seconds.....	69
<b>Table A.2</b> : Average Number of Stops per Vehicles.....	70
<b>Table A.3</b> : Average Speed in km/h.....	71
<b>Table A.4</b> : Average Stopped Delay per Vehicle in seconds. ....	72
<b>Table A.5</b> : Total Delay Time in h.....	73
<b>Table A.6</b> : Total Distance Traveled in km.....	74
<b>Table A.7</b> : Number of Stops.....	75
<b>Table A.8</b> : Number of Vehicles in the Network. ....	76
<b>Table A.9</b> : Number of Vehicles that have left the Network. ....	77
<b>Table A.10:</b> Total Stopped Delay in h.....	78
<b>Table A.11:</b> Total Travel Time in h. ....	79





## LIST OF FIGURES

	<u>Page</u>
<b>Figure 2.1</b> : Time-Space $(x, t)$ Domain [2].	5
<b>Figure 2.2</b> : Greenshields set up for field measurements and the instruments that he used [3].	7
<b>Figure 2.3</b> : The First Fundamental Diagram that Greenshields has offered [3].	7
<b>Figure 2.4</b> : The Bilateral Relationships of Traffic Variables [4].	8
<b>Figure 2.5</b> : Field Data obtained from [5].	8
<b>Figure 2.6</b> : A Comparison of Single-Regime Models from a Field Data from Istanbul [5].	11
<b>Figure 2.7</b> : A Discrete Moskowitz Function (Down) with the given Vehicle Trajectories (Up) [6].	12
<b>Figure 2.8</b> : The Road Segment between two consecutive Road Sections $x = x_0$ and $x = x_0 + L$ .	13
<b>Figure 2.9</b> : Moskowitz Function [7].	13
<b>Figure 2.10</b> : The Approximation of the Integral of $\rho(x, t)$ between $x = x_0$ and $x = x_0 + L$ .	14
<b>Figure 2.11</b> : The Jump Discontinuity on $\rho$ in $(x, t)$ -plane.	15
<b>Figure 3.1</b> : VSL Control in Istanbul [8].	22
<b>Figure 3.2</b> : Lane Allocation in Istanbul [9].	23
<b>Figure 4.1</b> : Discrete Highway Sections [10].	26
<b>Figure 4.2</b> : Line of Cars Moving on a Road.	27
<b>Figure 4.3</b> : A Curve for Illustrating Speed-Density Relationship proposed from Car-Following Model.	28
<b>Figure 4.4</b> : Density-Speed and Density-Flow Relationships proposed from Car-Following Model.	28
<b>Figure 4.5</b> : Vehicle Propagation based on Cell Automata Traffic Flow Model [10].	29
<b>Figure 4.6</b> : Macro-Meso-Microscopic Simulation Comparison [11].	29
<b>Figure 5.1</b> : Satellite Quicklook Image of the Study Field (Google Earth®).	31
<b>Figure 5.2</b> : Histogram for the Time Difference Data.	33
<b>Figure 5.3</b> : Flow Data for 8 Days.	33
<b>Figure 5.4</b> : Flow Data for 08.07.2010 (Thursday).	34
<b>Figure 5.5</b> : Flow Data (Up) HGV Composition for 08.07.2010 (Thursday) 14:45:28-23:48:56 (Down)	34
<b>Figure 5.6</b> : Wiedemann's Car Following Model [12].	36
<b>Figure 5.7</b> : Speed-Flow Calibration/Verification Results for Main Stream	38
<b>Figure 5.8</b> : Speed-Flow Calibration/Verification Results for Ramp	38

<b>Figure 5.9 :</b>	Speed-Flow Calibration/Verification Results for Whole Section .....	39
<b>Figure 5.10:</b>	Study Network generated in PTV VISSIM. ....	39
<b>Figure 5.11:</b>	Data Collection Point Locations.....	40
<b>Figure 5.12:</b>	Occupancy Rate Prediction Model.....	42
<b>Figure 5.13:</b>	No Control Density Profile.....	42
<b>Figure 5.14:</b>	Detector Locations.....	43
<b>Figure 5.15:</b>	Signal Head Locations.....	44
<b>Figure 5.16:</b>	Green Time Fluctuation with Respect to Occupancy Rate Measured for Ramp Metering Approach 1 (Cycle Time=20 sec, Minimum Green Time=10 sec).....	44
<b>Figure 5.17:</b>	Density Profile for Ramp Metering Approach 1 (Cycle Time=20 sec, Minimum Green Time=10 sec).....	45
<b>Figure 5.18:</b>	Green Time Fluctuation with Respect to Occupancy Rate Measured for Ramp Metering Approach 2 (Cycle Time=15 sec, Minimum Green Time=5 sec).....	45
<b>Figure 5.19:</b>	Green Time Fluctuation with Respect to Occupancy Rate Measured for Ramp Metering Approach 2 (Cycle Time=15 sec, Minimum Green Time=5 sec).....	46
<b>Figure 5.20:</b>	Desired Speed Decision Locations for Main Stream and Ramp. ....	47
<b>Figure 5.21:</b>	Desired Speed Decision Locations at the End of Network. ....	47
<b>Figure 5.22:</b>	Desired Speed Fluctuations for VSL Case 1 .....	50
<b>Figure 5.23:</b>	Desired Speed Fluctuations for VSL Case 2 at the Ramp.....	50
<b>Figure 5.24:</b>	Desired Speed Fluctuations for VSL Case 2 at the Main Stream.....	51
<b>Figure 5.25:</b>	Desired Speed Fluctuations for VSL Case 3 .....	51
<b>Figure 5.26:</b>	Desired Speed Fluctuations for VSL Case 4 .....	51
<b>Figure 5.27:</b>	Density Profile for VSL Case 1. ....	52
<b>Figure 5.28:</b>	Density Profile for VSL Case 2. ....	52
<b>Figure 5.29:</b>	Density Profile for VSL Case 3. ....	53
<b>Figure 5.30:</b>	Density Profile for VSL Case 4. ....	53

# **MICROSCOPIC SIMULATION OF DYNAMIC FREEWAY TRAFFIC FLOW CONTROL APPROACHES ON AN URBAN HIGHWAY**

## **SUMMARY**

In this thesis, firstly traffic flow theories are mainly introduced in macroscale which forms the basis of the most of the simulation studies and control strategies. Then relationship between the traffic variables are demonstrated and the flow theories based on the hydraulic model are analyzed and the shockwaves which are the main reason of the traffic congestion shown analytically. Thereafter, main criticism about these models are discussed and improvements are summarized. In the third section of this study macro-micro-mesoscopic simulation models are described and later in the fourth section traffic control approaches are explained.

In the application part of this study, the study field is introduced. Data collection methods from RTMS (Remote Traffic Microwave Sensor) are briefly explained and the data methodology is expressed. Moreover, the microsimulation program PTV VISSIM is described and longitudinal and lateral movement models are described. Calibration method is described which demonstrates the validation of the simulation. For dynamic ramp metering approach two cases of ALINEA algorithm are proposed and for VSL approaches four cases are proposed. The fluctuations of the green time for ramp metering and the speed limits for VSL is plotted. Also density profiles for each approach is selected. At the end, results are discussed for various performance indicators such as total travel time, average delay time per vehicle, average number of stops per vehicle, etc.



# **KENT İÇİ ÇEVREYOLLARINDA DİNAMİK TRAFİK AKIM KONTROL YAKLAŞIMLARININ MİKRO ÖLÇEKLİ SİMÜLASYONU**

## **ÖZET**

İstanbul gibi büyük metropollerde trafik sorunu her zaman büyük sorun olmuştur. Yüksek seyahat süreleri, randevulara gecikmeler, dur kalklar ve dur kalklara bağlı çevreye salınan zararlı emisyon gazları trafik sıkışıklığından doğan önemli sorunların başlarında gelmiştir.

Geometrik düzenlemeler, statik sayımlara bağlı statik çözümler gibi geleneksel trafik sıkışıklığı çözüm yöntemleri günümüze dek önemli çözüm yöntemleri arasında yer almıştır. Oysaki trafik talebi değil yıllık; aylık, günlük, saatlik hatta ve hatta dakikalık değişimler göstermekte, dolayısıyla statik çözümler veya geometrik çözümler zaman zaman çözüm getirmemektedir.

Bilgisayar bilimlerinin, elektroniğin ve teknolojinin gelişmesi ile birlikte bu statik çözümlerin yerini trafiğe anlık tepkiler verebilen akıllı ulaşım sistemleri adı verilen sistemler geliştirilmeye başlanmıştır. Akıllı ulaşım sistemleri kapsamında çözümler gerçekleştirilirken simülasyon programları trafik mühendislerinin kararlarında yol gösterici olmuştur. Simülasyon programları arkasındaki modelin detay seviyesine göre ölçeklendirilmiştir. Aynı şekilde trafik mühendislerinin akıllı ulaşım sistemleri kapsamında problem çözümlerinde kullandıkları kontrol yapıları da aynı simülasyon gibi detay seviyesine göre ölçeklendirilmiştir.

Bu çalışmada, öncelikle hem simülasyon çalışmalarının hem de kontrol yapılarının temelini oluşturan trafik akım teorileri makro ölçekte tanıtılmıştır. Ardından trafik akım değişkenleri arasındaki bağıntı gösterilmiş, saha çalışmalarından yapılan örnekler gösterilmiş ve literatürdeki diğer bağıntılar özetlenmiştir. Trafik akım teorisinin hidrolik model olarak makro ölçekli modelleri incelenmiş ve trafik sıkışıklığının önemli bir sebebi olan şok dalgaları analitik olarak analiz edilmiştir. Ardından hidrolik modelin eksik yanlarına olan eleştiriler ele alınmış ve ortaya atılan gaz kinematiği modelleri özetlemiştir.

Bir sonraki kısım olan üçüncü kısımda çalışma sahasında uygulanacak trafik kontrol yaklaşımları özetlenmiştir. Uygulamada kullanılan model tahmini yapan kontrol yapısının genel literatür özeti yapılmıştır. Ardından katılım kontrolü yaklaşımları tanıtılmıştır. Katılım kontrolü yaklaşımları yerel katılım kontrol stratejileri ve sistem geneli katılım kontrol stratejileri olarak iki ana grup altında toplanmıştır. Daha sonra değişken hız limiti yaklaşımı hakkında ön bilgi verilmiştir. Son olarak ise tezde kullanılsa da şerit tahsisi ve kapanması gibi uygulamalardan da kısaca söz edilmiştir.

Çalışmanın dördüncü kısmında, makro ölçekli trafik simülasyon modelleri tanıtılmıştır. Daha sonra bu çalışmanın önemli çıktılarından mikro ölçekli trafik

simülasyon programlarının arkasındaki taşıt takip modelinin matematiksel temelleri incelenmiştir. Mikro ölçekli simülasyon programlarının makro ölçekli simülasyon programlarından farkı olan birim taşıtların dinamiği ortaya konulmuş ve Newton'un etki tepki yasasına analogi yapılmak suretiyle belli bir hassasiyete bağlı taşıtların öndeki araç ile hız farkının azalmasına veya artmasına bağlı olarak ivmesinin değişimini gösteren temel diferansiyel denklem ortaya konup çözülüp buradan yoğunluk-hız ilişkisi ve yoğunluk akım ilişkisi gösterilmiştir. Ardından mezo ölçekli trafik akım modelleri özetlenmiştir.

Çalışmanın uygulama kısmı olan beşinci kısım için öncelikle uygulama sahası tanıtılmıştır. Daha sonra RTMS (Remote Traffic Microwave Sensor-Uzaktan Mikrodalga Trafik Algılayıcısı) tanıtılarak sahadan elde edilen verilerin dağılımlarının analizi yapılmıştır.

Sahadan toplanan verilerin birleştirilme yöntemi kısaca anlatılıp katılım ve ana kol için simülasyon programına girilecek taşıt girdileri ile taşıt kompozisyonları belirlenmeye çalışılmıştır.

Ardından mikro ölçekli trafik simülasyon programı PTV VISSIM kısaca tanıtılmıştır. Enlemesine ve boylamasına hareket modelleri analiz edilip Wiedemann'ın PTV VISSIM simülasyon programında kullanılan taşıt takip modeli anlatılmıştır. Ardından network elemanları tanıtılmak suretiyle simülasyon ortamının nasıl çalıştığı anlatılmaya çalışılmıştır. Mikro ölçekli trafik simülasyonlarının geçerliliği için önemli bir kriter olan kalibrasyon yöntemleri gösterilmiştir.

Dinamik trafik akım kontrolü yaklaşımları ile karşılaştırılması ve dedektör üzerindeki taşıtların toplam işgal sürelerinin tahmini için kontrolsüz durum testleri gerçekleştirilmiştir. Bunun için oluşturulan regresyon modeli ortaya konularak önceki çevrimler için katsayılar elde edilmiştir. Bu bağlamda son olarak kontrolsüz durumun yoğunluk profili çizilerek zamana bağlı değişimine bakılmıştır.

Daha önceden belirtilen dinamik trafik akım kontrolü yaklaşımlarından ilki olan katılım kontrolünün literatürde nasıl yapıldığı kısaca anlatılarak parametreler tanıtılmıştır. Yaklaşımlar için yazılan VAP (Vehicle Actuated Programming-Taşıt Uyarımlı Programlama) kodunun çalışması için yerleştirilen dedektörün ve sinyallerin yerleri belirtilmiştir. Ardından bu yaklaşım için de denenen çevrim sürelerine ve minimum yeşil ışık sürelerine bağlı olarak akıntı aşağı kısımdaki taşıt işgal oranlarının nasıl değiştiği ve buna bağlı olarak her iki durumda da aynı segmentin yoğunluk profillerinin nasıl değiştiği gözlemlenmiştir.

Dinamik trafik akım kontrolü yaklaşımlarından ikincisi olan değişken hız yönetimi için de limit hız işaretinin konulduğu yerler belirtilmiştir. Ardından parçalı fonksiyon şeklinde taşıt işgal oranlarına, doğal olarak da zamana bağlı değişen gösterilecek hız modeli önerilmiştir. Bunun için dedektör işgal oranları ve gösterilecek hızlar için 4 adet durum belirtilip test sonuçlarına bakılmıştır. Ardından katılım kontrolünde olduğu gibi işgal oranlarının değişimine bağlı olarak hız limitleri nasıl değiştiği her bir durum için gözlemlenmiştir. Yine katılım kontrolü yaklaşımında olduğu gibi belirtilen 4 duruma bağlı olarak akım aşağı yol segmentinin yoğunluk profilleri incelenmiştir.

En son bölümde taşıtların rastgele gelişlerinin çoklu çalıştırmalar sonucu değişimleri değerlendirilmiştir. Performans ölçütü olarak ortalama taşıt başına gecikme süreleri,

ortalama taşıt başına dur kalk sayıları, ortalama taşıt başına dur kalklardan kaynaklı gecikme süreleri, toplam gecikme süreleri, toplam dur kalk sayıları, toplam dur kalklardan kaynaklı gecikme süreleri, toplam seyahat süreleri ve araçların ortalama hızları seçilmiş ve bunların her bir kontrol yaklaşımındaki değişimleri incelenmiştir. Son olarak gelecek çalışmalar için yön gösterilmiştir.





## **1. INTRODUCTION**

Transportation has been always an important problem during the civilized era of the mankind. Since humans are socialized creatures, there have been always a transportation demand among communities. After the invention of the automobile, various problems have been troubled by people.

Until the early 20s, due to the insufficient technological improvements, all the control approaches of transportation demand have been performed by static data observed from field at a certain time. In the light of developments in computer science, control theory and electronics, data observation can be executed more frequently and control of the transportation systems as well as traffic can be done dynamically.

Intelligent Transport Systems (ITS) are systems which optimize the user or system utility by executing smart algorithms with the aid of software and hardware devices real-time or frequently. In [13], ITS is defined similarly. ITS are the systems maximizing efficiency while minimizing risks through the tools of traffic engineering, software, hardware and communications technologies. On the other hand, technology is combined via advanced mathematical methods with the conventional transportation infrastructure [14].

### **1.1 Statement of the Problem**

Traffic congestion and management have been an important problem for various engineering branches, because traffic is dependent on several parameters such as geometry of the road, desired speed of the cars, hour of day, day of week, weather conditions and so on. . . Most of them are more or less managed with different traffic control techniques.

On the other hand, when an optimal control problem is concerned, a utility function should be optimized with the given parameters. In traffic engineering, this can be travel

time [15], flow at a section, density of a segment, average delay of vehicles, number of stops per vehicle or level of service (LOS) etc.

Like the other metropolitan cities in the world, Istanbul has been suffering traffic congestion problems through years. The main corridors, especially the corridors including Boğaziçi and Fatih Sultan Mehmet (FSM) Bridges, have a high degree of traffic demand and volume not only during the peak hours but also during other hours of day. An important factor for the traffic congestion among these corridors is the high demand at the feeders, which is called ramp in traffic engineering literature.

For improving traffic flow two main methods are came into prominence. Ramp metering is the first method for that which aims to smooth the flow by controlling ramp with a signal. However there are some concerns about the social effects of this method. Because of the negative effects on the drivers at the ramp, there are some scholars arguing ramp metering [16]. Second, speed control is also applied extensively to prevent the shock waves in traffic, which will be discussed in Section 2. On the other hand, there may be some doubts that speed restrictions will not work because there is a tendency of violation of speed restrictions in Istanbul. Nevertheless, there are some studies showing that the usage of EDS (Elektronik Denetleme Sistemi-Turkish for “Electronic Violation Detection System”) highly reduces the violation [17].

## **1.2 Objectives**

The main purpose of this study is to seek for a solution to the congestion problem on the Levent Ramp of Istanbul Outer Beltway (O-2) on which FSM Bridge is located. In order to perform this objective ramp metering and speed management approaches are tried. These control approaches are done dynamically according to the traffic data. Vehicle actuated algorithms are performed during the dynamic approaches. Performance indexes such as total travel time, flow at a section, density of a segment, average delay of vehicles, number of stops per vehicle are demonstrated to see the efficiency of the approaches.

### 1.3 Literature Overview

The studies, which the author of this study is inspired from, are [18] and [4]. This study is considered and planned after the conversation with the authors. In [18], an arterial in Beşiktaş, Istanbul is analysed and tried to be controlled dynamically with VAP (Vehicle Actuated Programming) module of PTV VISSIM (Planung Transport Verkehr Verkehr In Städten SIMulationsmodell-German for “Planning Transport Traffic Traffic in Cities Simulation Model) software. The most popular control approach for the ramp is proposed by Papageorgiou et al. in 1991 [19]. Another traffic flow control approach by lumped parameter system is made in [4]. In the same study, a dynamic and coordinated ramp metering mechanism is dealt with various scenarios by the discretization of LWR (Lighthill-Whitham-Richards) model on [20] [21] which will be discussed in Section 2. There are also numerical investigations on LWR Theory. In Transportation Engineering literature Cell Transmission Model [22], in Mathematics literature Godunov’s Scheme [23] approaches with the concept of mesh, however there are also grid free solutions as in [6].



## 2. TRAFFIC FLOW

Traffic flow is gerally considered on a one-dimensional way of moving vehicles. In order to explain traffic flow, there is a need of a brief explanation of traffic variables.

### 2.1 Traffic Variables

In microscopic point of view of traffic flow, the vehicles can be represented by their position and time. In traffic engineering these are called the trajectories [7] of the vehicles. On the other hand in LWR Theory they are the characteristics of the solution of a wave function [24].

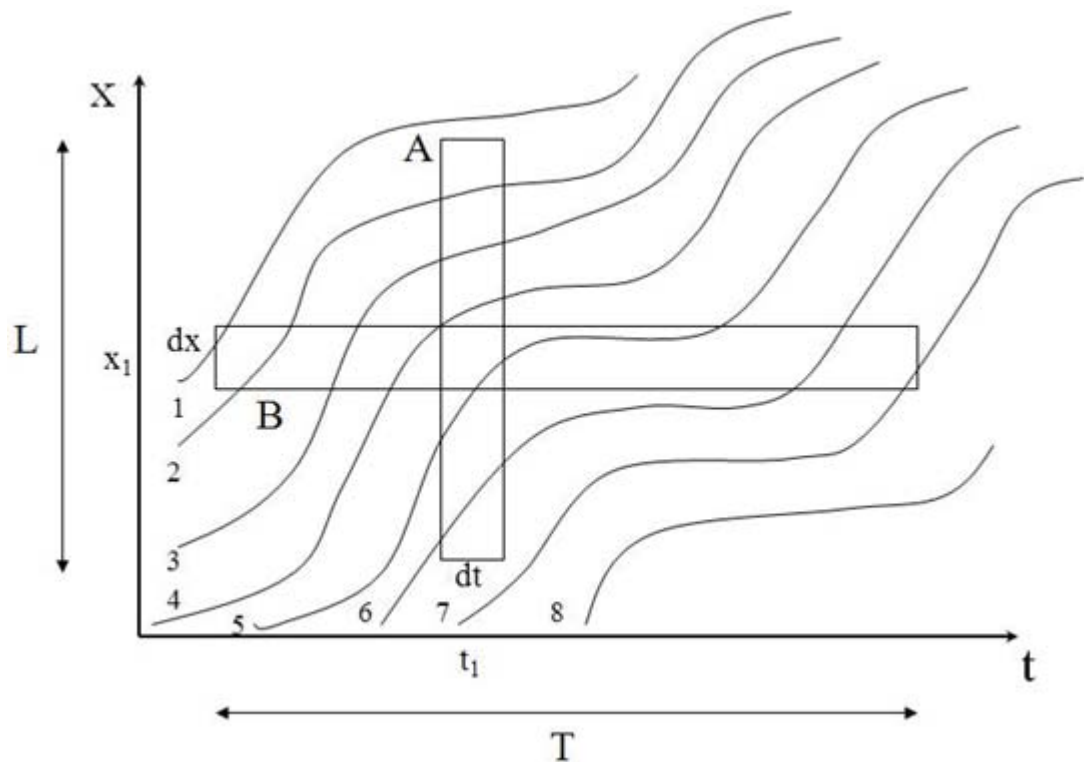


**Figure 2.1:** Time-Space  $(x, t)$  Domain [2].

These variables are important while defining the macroscopic variables of traffic flow, which are density, speed and flow.

### 2.1.1 Density

Density is defined as the instantaneous number of vehicles exists at a certain length of road. Sometimes it is better to used occupancy or occupancy rate of the detector on a field, because of the difficulties to measure density. In broader case, concentration is used for both of them [25]. A common mathematical formula for density, denoted as  $\rho$ , is

$$\rho = \frac{n_x}{L} = \frac{n_x dt}{L dt} \quad (2.1)$$

where  $n_x$  denotes the number of vehicles in the road section which has a length of  $L$  represented in Figure 2.1.

### 2.1.2 Flow

The number of vehicles passed at a highway intersection at a certain time (generally an hour) is called flow. In traffic counts, number of vehicles, which is called traffic volume, is counted in a precise time interval which is less than an hour (in consensus 15 min [26]). The maximum value of the vehicle counts converted into one hour is called flow rate, which can be seen as an analogy to the blood pulse measured less than a minute but converted into minutely time span. The general formula for flow  $q$  is

$$q = \frac{n_t}{T} = \frac{n_t dx}{T dx} \quad (2.2)$$

where  $n_t$  denotes the number of vehicles passed at a highway intersection in a certain time interval  $T$  which can be seen in Figure 2.1.

### 2.1.3 Speed

When speed<sup>1</sup> is mentioned in traffic flow theory, it is generally referred to space-mean speed or precisely weighted mean of speeds of the vehicles to cross a distance, because speed denotes the length of road that a vehicle travels in a certain time interval. This is mentioned in [20] but referred to [27]. So, the mean speed is

$$u = \frac{n_x}{L} = \frac{n_t dx}{T dx} \quad (2.3)$$

---

<sup>1</sup>Here speed denotes the stream speed.

where  $n_x$  denotes the number of vehicles in the road section which has a length of  $L$  and  $t_i$ 's are the time to cross  $L$  for vehicle  $i$ .

## 2.2 Relationship Between the Traffic Variables: MFD

The relationship between the traffic variables roots back to the study of Greenshields made in [28]. Here there are some pictures about the measurements that he made in Figure 2.2.

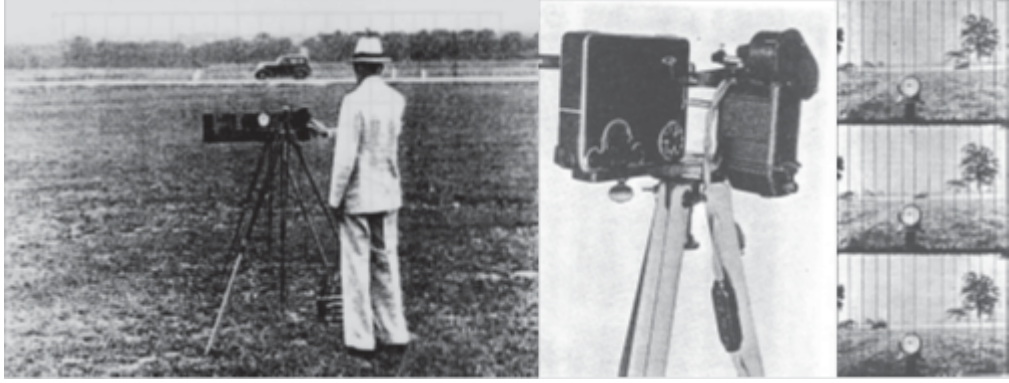


**Figure 2.2:** Greenshields set up for field measurements and the instruments that he used [3].

Then he has come up with the idea of a linear relationship between density and speed

$$u = u_f \left( 1 - \frac{\rho}{\rho_j} \right) \quad (2.4)$$

where  $u_f$  denotes the free flow speed and  $\rho_j$  denotes the jam density. The results that he found are shown in Figure 2.3.

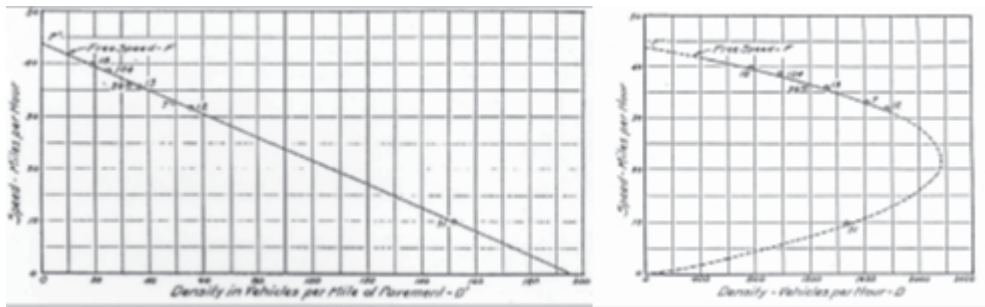


**Figure 2.3:** The First Fundamental Diagram that Greenshields has offered [3].

Generally the main relationship of traffic flow is considered as

$$q = u(\rho)\rho. \quad (2.5)$$

The bilateral relationships among density-speed, flow-speed and density-flow are demonstrated in Figure 2.4 and scatter plots from the field observations made in [5] are shown in Figure 2.5.

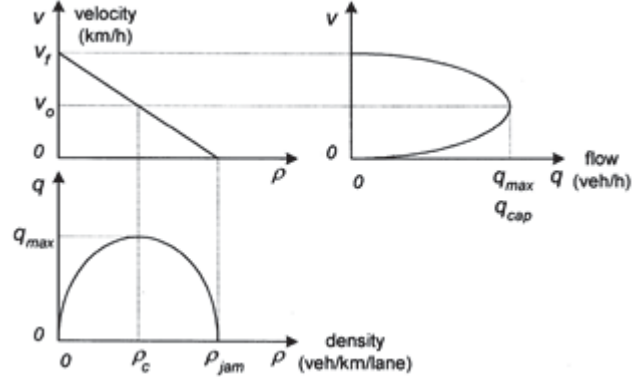


**Figure 2.4:** The Bilateral Relationships of Traffic Variables [4].

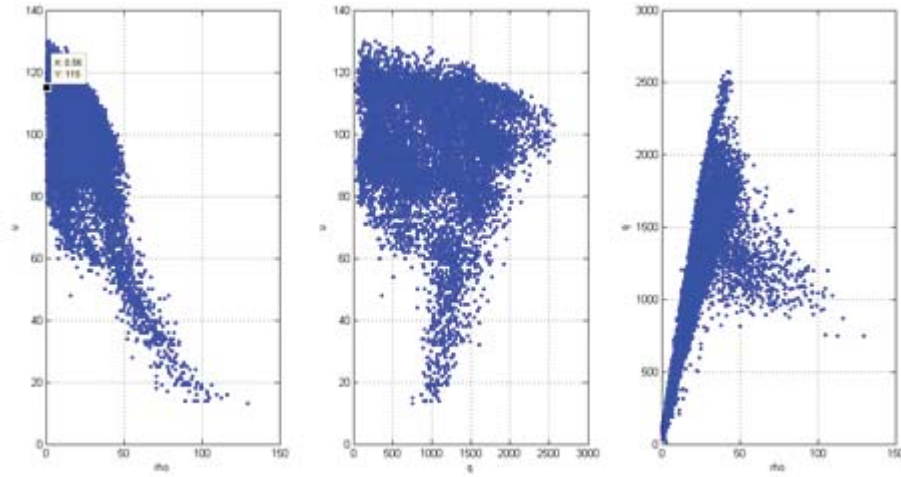


**Figure 2.5:** Field Data obtained from [5].

Later, various relationships offered by various scholars. There are two tendencies in representing the MFD. A brief summary of single-regime and multi-regime models are presented in [1] and [5].



**Table 2.1:** Single-Regime Models [1].

Model	Relationship
Greenshields Model (1935)	$u = u_f \left( 1 - \frac{\rho}{\rho_j} \right)$
Greenberg Model (1959)	$u = u_0 \ln \left( \frac{\rho_j}{\rho} \right)$
Underwood Model (1961)	$u = u_f e^{\left( -\frac{\rho}{\rho_j} \right)}$
Newell Model (1965)	$u = u_f \left( 1 - e^{\left( \frac{\lambda}{v_f} \left( \frac{1}{\rho} - \frac{1}{\rho_j} \right) \right)} \right)$
Northwestern Model (1967)	$u = u_f e^{\left( -\frac{1}{2} \left( \frac{\rho}{\rho_j} \right)^2 \right)}$
Pipes-Munjial Model (1967)	$u = u_f \left( 1 - \left( \frac{\rho}{\rho_j} \right)^n \right)$
Modified Greenshields Model (1994)	$u = u_0 + (u_f - u_0) \left( 1 - \left( \frac{\rho}{\rho_j} \right)^\alpha \right)$
Kerner-Kornhäuser Model (1994)	$u = u_f \left( \frac{1}{\left( 1 + e^{\left( \frac{\frac{\rho}{\rho_0} - 0.25}{0.06} \right)} \right)} - 3.72 \times 10^{-6} \right)$
Del Castillo Model (1995)	$u = u_f \left( 1 - e^{\frac{ c_j }{u_f} \left( 1 - \frac{\rho_j}{\rho} \right)} \right)$
Van Ärde Model (1995)	$\rho = \frac{1}{c_1 + \frac{c_2}{u_f - u} + c_3 u}$
MacNicholas Model (2008)	$u = u_f \left( \frac{\rho_j^n - \rho^n}{\rho_j^n + m \rho^n} \right)$

**Table 2.2:** Multi-Regime Models [1].

Model	Free-Flow	Transitional-Flow	Congested-Flow
Ede Model	$u = 54.9e^{-\frac{\rho}{163.9}}$ where $\rho \leq 50$		$u = 54.9\ln\left(\frac{192.5}{\rho}\right)$ else
Two-Regime Model	$u = 60.9 - 0.515\rho$ where $\rho \leq 65$		$u = 40 - 0.265\rho$ else
Modified Greenberg Model	$u = 48$ where $\rho \leq 50$		$u = 32\ln\left(\frac{145.5}{\rho}\right)$ else
Three-Regime Linear Model	$u = 50 - 0.098\rho$ where $\rho \leq 40$	$u = 81.4 - 0.913\rho$ where $40 \leq \rho \leq 65$	$u = 40 - 0.265\rho$ else

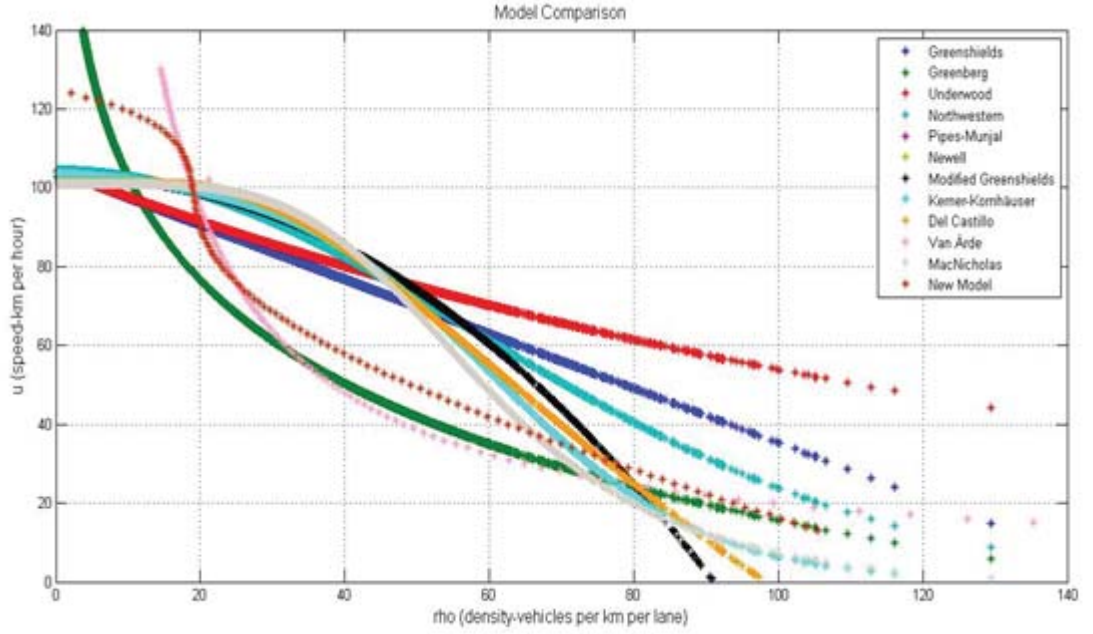


**Figure 2.6:** A Comparison of Single-Regime Models from a Field Data from Istanbul [5].

The need of multi-regime models came from the lack of fitness of single-regime models to whole the empirical data, since multi-regime models are better in fitting to the field observation data than single-regime models. On the other hand, multi-regime models demonstrate the nature of the field data, i.e. single-regime models are much better than the multi-regime models to demonstrate the nature of the physical event. So, there is a trade of between the empirical observations and mathematical elegance.

### 2.3 Hydraulic Model: Lighthill-Whitham-Richards (LWR) Equation

Generally, when LWR Equation is concerned, [20] and [21] are referenced which is generated from the law of conservation. This is based on the assumptions that the total number of vehicles are conserved and the speed is a function of density.

In time-space domain, if we take the derivative of the position of a vehicle we obtain its velocity by definition.

$$u(x, t) = \frac{dx}{dt}. \quad (2.6)$$

If this result is combined with (2.5), (2.6) yields

$$\frac{dx}{dt} = \frac{q(x,t)}{\rho(x,t)} \Rightarrow \int_{t_0}^{t_0+T} q(x,t) dt = \int_{x_0}^{x_0+L} \rho(x,t) dx. \quad (2.7)$$

Here it is needed to introduce a function which is called cumulative number of vehicles function, also called Moskowitz function, shown as  $N(x,t)$ . However, this function is nothing but function representation of  $n_t$  variable, introduced in Section 2.1.1. This function gives the total number of vehicles, as it can be inferred from its name, at a certain location and time. A good representation of this function with given vehicle trajectories is shown in Figure 2.7.

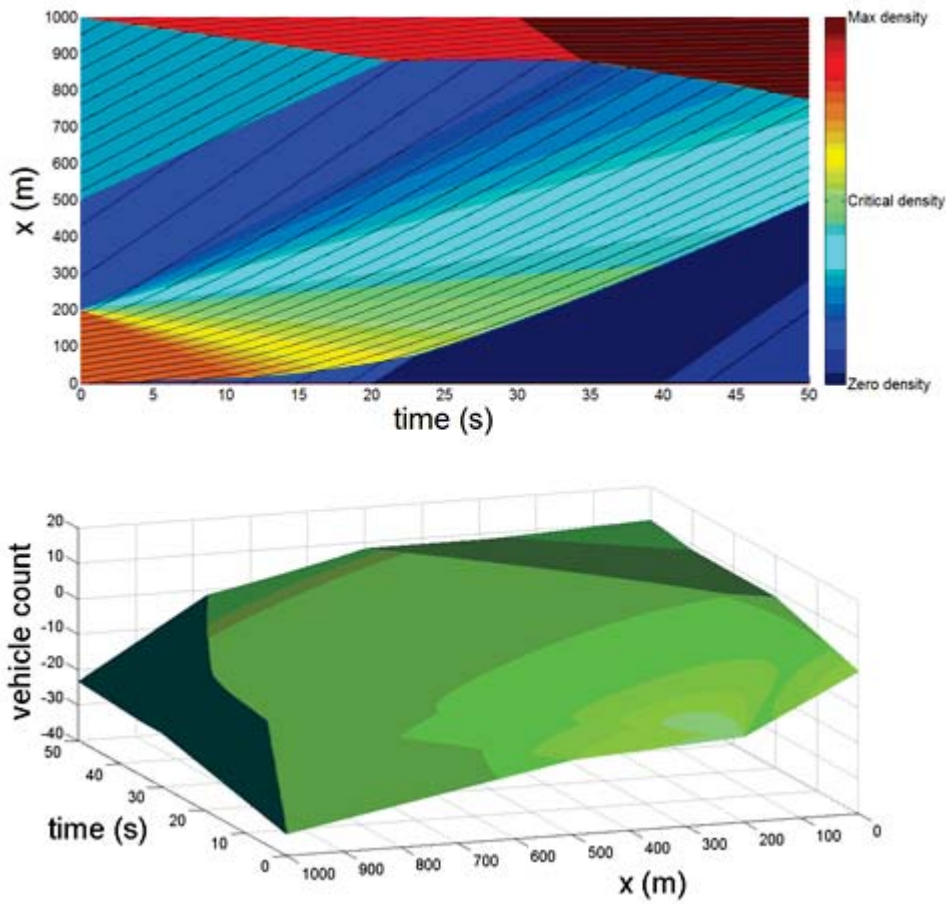


**Figure 2.7:** A Discrete Moskowitz Function (Down) with the given Vehicle Trajectories (Up) [6].

This function is important to introduce since density and flow can be derived thereof. Because of the assumption that the number of vehicles is conserved, the difference of vehicles between the road sections  $x = x_0$  and  $x = x_0 + L$ , which can be seen in Figure

2.8, is obtained from the derivative of the Moskowitz function w.r.t. time, i.e.

$$\frac{dN}{dt} = q(x_0, t) - q(x_0 + L, t). \quad (2.8)$$

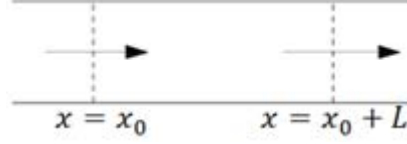


**Figure 2.8:** The Road Segment between two consecutive Road Sections  $x = x_0$  and  $x = x_0 + L$ .

This can also be seen in Figure 2.9.

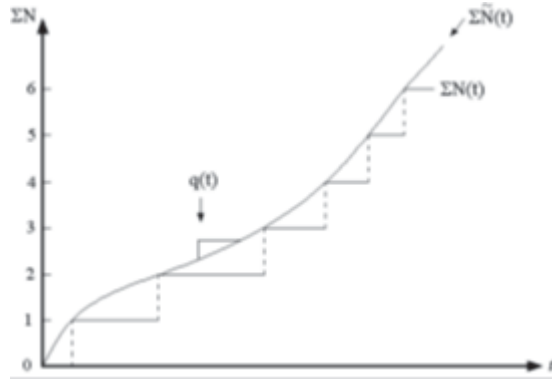


**Figure 2.9:** Moskowitz Function [7].

Conversely, if  $q$  is integrated along a time interval  $T$ , from  $t = t_0$  to  $t = t_0 + T$ ,  $N(x, t)$  is obtained

$$N = \int_{t_0}^{t_0+T} q(x, t) dt. \quad (2.9)$$

The left hand side of the Equation (2.7) will be  $N$ , so

$$N = \int_{x_0}^{x_0+L} \rho(x, t) dx. \quad (2.10)$$

When the  $N$  in Equation (2.10) is substituted with the  $N$  in Equation (2.8),

$$\frac{d}{dt} \int_{x_0}^{x_0+L} \rho(x, t) dx = q(x_0, t) - q(x_0 + L, t). \quad (2.11)$$

Here the full derivative is replaced with the partial derivative by calculating the total derivative since  $x_0$  and  $x_0 + L$  does not depend on time. Dividing both parts to  $L$  and

taking limit as  $L \rightarrow 0$ :

$$\begin{aligned}
\lim_{L \rightarrow 0} \frac{\partial}{\partial t} \frac{1}{L} \int_{x_0}^{x_0+L} \rho(x, t) dx &= \lim_{L \rightarrow 0} \frac{q(x_0, t) - q(x_0 + L, t)}{L} \\
&= - \lim_{L \rightarrow 0} \frac{q(x_0 + L, t) - q(x_0, t)}{L} \\
&= - \frac{\partial q(x_0, t)}{\partial x_0}.
\end{aligned} \tag{2.12}$$

Calculating the integral demonstrated in Figure 2.11,

$$\lim_{L \rightarrow 0} \frac{1}{L} \int_{x_0}^{x_0+L} \rho(x, t) dx = \rho(x_0, t). \tag{2.13}$$

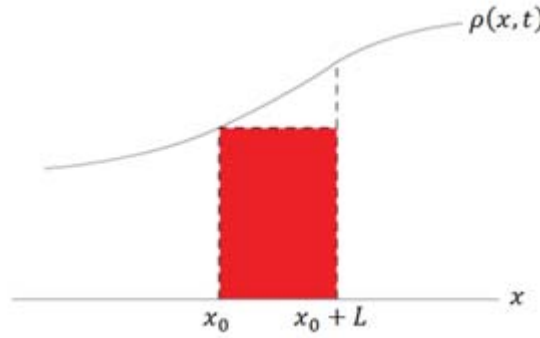


**Figure 2.10:** The Approximation of the Integral of  $\rho(x, t)$  between  $x = x_0$  and  $x = x_0 + L$ .

By replacing  $x_0$  with  $x$  and combining the result obtained from the Equation (2.13) and Equation (2.12), the well-known LWR Equation is obtained

$$\frac{\partial \rho(x, t)}{\partial t} + \frac{\partial q(x, t)}{\partial x} = 0. \tag{2.14}$$

The LWR Equation is an analogy to the differential form of the continuity equation in physics. It says that if there is an increase at the particle density in a segment at an instantaneous time, there should be a flow into that segment. Moreover, if there is an outgoing flow at a section in a time interval, the particle density will decrease.

## 2.4 Notes on Shock Waves

In [27], it is stated that shock occurs as discontinuities in  $\rho$ . Here the discontinuities describes the situation of a sudden transition from low density to high density. Let

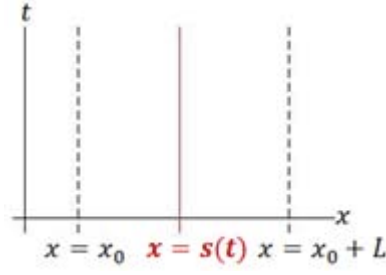


**Figure 2.11:** The Jump Discontinuity on  $\rho$  in  $(x, t)$ -plane.

us consider a jump discontinuity at a certain road section  $x = s(t)$  which varies with respect to time where  $x_0 \leq s(t) \leq x_0 + L$ .

Let us assume  $p, q \in C^1$  in  $x_0 \leq x < s(t)$  and  $s(t) < x \leq x_0 + L$ . In this case Equation (2.11) changes as

$$\frac{d}{dt} \int_{x_0}^{s(t)} \rho(x, t) dx + \frac{d}{dt} \int_{s(t)}^{x_0+L} \rho(x, t) dx = q(x_0, t) - q(x_0 + L, t). \quad (2.15)$$

Here the boundaries of the integrals depend on time, that is why there is a need to calculate total derivatives

$$\begin{aligned} \frac{d}{dt} \int_{x_0}^{s(t)} \rho(x, t) dx &= \frac{\partial}{\partial t} \int_{x_0}^{s(t)} \rho(x, t) dx + \frac{dx}{dt} \left[ \rho(s^-, t) \frac{ds}{dx} - 0 \right], \\ \frac{d}{dt} \int_{s(t)}^{x_0+L} \rho(x, t) dx &= \frac{\partial}{\partial t} \int_{s(t)}^{x_0+L} \rho(x, t) dx + \frac{dx}{dt} \left[ 0 - \rho(s^+, t) \frac{ds}{dx} \right]. \end{aligned} \quad (2.16)$$

Here  $s^+$  and  $s^-$  represents the values of  $x$  in front of the shock and back of the shock respectively. Recall that

$$\frac{ds}{dx} = \frac{ds}{dt} \frac{dt}{dx} = \dot{s} \frac{dt}{dx}$$

so Equations in (2.16) will be

$$\begin{aligned} \frac{d}{dt} \int_{x_0}^{s(t)} \rho(x, t) dx &= \frac{\partial}{\partial t} \int_{x_0}^{s(t)} \rho(x, t) dx + \rho(s^-, t) \dot{s}, \\ \frac{d}{dt} \int_{s(t)}^{x_0+L} \rho(x, t) dx &= \frac{\partial}{\partial t} \int_{s(t)}^{x_0+L} \rho(x, t) dx - \rho(s^+, t) \dot{s}. \end{aligned} \quad (2.17)$$

Here by  $\dot{s}$  has a physical meaning and it represents the shock velocity. If  $x_0 \rightarrow s^-$  and  $x_0 + L \rightarrow s^+$  the integrals vanishes and from Equation (2.15)

$$\dot{s} = \frac{q(s^+, t) - q(s^-, t)}{\rho(s^+, t) - \rho(s^-, t)}. \quad (2.18)$$

From this result, it can be observed that the shock velocity is related to the fraction of the flow difference between front and back sides of the shock and the density difference between front and back sides of the shock.

## 2.5 Improvements on LWR Equation

Although LWR Equation satisfacts the analytical transactions, a need for a new model is emerged to meet the empirical results. That is why, LWR Equation is improved by Payne in 1971 [29]. The model that Payne developed was based on two traffic conditions: free flow seen in low densities and congested flow seen in high densities

$$\begin{cases} \frac{\partial \rho}{\partial t} + \frac{\partial(\rho u)}{\partial t} = 0 \\ \frac{\partial(\rho u)}{\partial t} + \frac{\partial(\rho u^2 + p(\rho))}{\partial t} = 0 \end{cases} \quad (2.19)$$

where congested flow regime is valid. Here  $p$  symbolizes a pressure term which stands for an analogy to gas dynamics and is a function of  $\rho$ . However, this model has also been critisized by Daganzo [30]. The main criticism of this model was, this model does not fulfill two main assumptions of traffic flow, i.e. no information travels faster than cars and density and velocity should be non-negative and bounded.

Aw and Rascle [31] have improved the theory that Payne have suggested by changing the spatial derivative  $\partial/\partial x$  with the convective derivative  $\partial/\partial t + u\partial/\partial x$ , which stands for a derivative taken on a moving coordinate system, in second equation

$$\begin{cases} \frac{\partial \rho}{\partial t} + \frac{\partial(\rho u)}{\partial t} = 0 \\ \frac{\partial(\rho(u+p(\rho)))}{\partial t} + \frac{\partial(\rho u(u+p(\rho)))}{\partial t} = 0. \end{cases} \quad (2.20)$$

An alternative model is proposed by Colombo [32]

$$\begin{cases} \frac{\partial \rho}{\partial t} + \frac{\partial(\rho u)}{\partial t} = 0 \\ \frac{\partial q}{\partial t} + \frac{\partial((q-Q)u)}{\partial t} = 0 \end{cases} \quad (2.21)$$



where  $Q$  corresponds to a parameter of the road and  $q$  is the flow (weighted) which is equivalent to the linear momentum in gas dynamics. An advanced mathematical analysis of these models are made in [33], [34] and [35].



### **3. TRAFFIC CONTROL APPROACHES**

In order to reduce the traffic congestion and control the traffic flow in an optimal state various approaches are made by traffic engineers. Since increasing the capacity of a highway may not be possible in every case, smart control systems are proposed by various scholars. In this study, ramp metering and variable speed limit controls are tested in order to propose a solution to the congestion problem at the Levent Ramp of the Istanbul Outer Beltway. There are also lane closure or allocation approaches, however it is not in the scope of this study, because there is no two way data available for the study section.

The control systems are made in three ways. Firstly, these methods are applied statically which means the output of the control system does not change with respect to input or any other parameters (independent variables). Secondly, the control mechanism varies with respect to time which is called time dependent control system or pretimed control system. The last type of control systems is dynamic control systems. These type of control is made by adjusting the output by controlling the given input. In traffic control systems generally traffic control is made by the occupancy rate measured by the detectors. This type of traffic control is also called traffic responsive control system.

In this study, model predictive control is made in order to prevent congestion from three consecutive cycles. In this section; firstly, model predictive control is explained. Then, traffic control approaches ramp metering, variable speed limit and lane closure are introduced in order to give a background to the study.

#### **3.1 Model Predictive Control (MPC)**

MPC models predict the change in the dependent variables of the modeled system that will be caused by changes in the independent variables. MPC is an optimal control method applied in a rolling horizon framework. Optimal control has been successfully

applied by several researchers in traffic control over the years [36]. Either optimal control or MPC have the advantage that the controller generates control decisions that are optimal according to a controller-supplied objective function. However, MPC offers some important advantages over conventional optimal control. First, optimal control has an open-loop structure, which means that the disturbances (in our case: the traffic demands) have to be completely and exactly known before the simulation, and that the traffic model has to be very accurate to ensure sufficient precision for the whole simulation. MPC operates in closed-loop, which means that the traffic state and the current demands are regularly fed back to the controller, and the controller can take disturbances into account and correct for prediction errors resulting from model mismatch. Second, adaptivity is easily implemented in MPC, because the prediction model can be changed or replaced during operation. This may be necessary when traffic behavior significantly changes (e.g., in case of incidents, changing weather conditions, lane closures for maintenance). Third, for MPC a shorter prediction horizon is usually sufficient, which reduces complexity, and makes the real-time application of MPC feasible [37]. In this study a linear regression model is used to predict the occupancies of the next time frame, which will be explained in Section 5.3.

## **3.2 Traffic Control Approaches**

### **3.2.1 Ramp metering**

Ramp Metering (or Flow Signals) is a control mechanism for optimizing traffic flow at the downstream section of a highway with a signal at the ramp [38]. There are three main purposes for using ramp metering:

- control the number of vehicles that are allowed to enter the freeway,
- reduce the freeway demand at the downstream section and
- reducing congestion by decreasing the vehicle weaving (platooning) possibility.

In [39], ramp metering strategies are categorized as their level of scope ramp metering which are

- local ramp metering (isolated) and
- systemwide (coordinated) ramp metering.

Some ramp metering strategies for local ramp metering and systemwide ramp metering are presented in this section.

#### **3.2.1.1 Local (Isolated) ramp metering control strategies**

Local ramp metering is a control system which deals with an isolated highway section rather than the whole network. Some local ramp metering strategies are summarized in four types [39].

- Demand Capacity Control: In this type of control system metering rate is determined by the upstream volume and downstream capacity. The difference between the upstream volume and downstream capacity determines the metering rate for the next cycle.
- Upstream Occupancy Control: In this strategy, real-time occupancy upstream of the on-ramp is used in order to determine the metering rate for the next cycle.
- Gap-Acceptance Control: For gap acceptance control, occupancy measurements from upstream of the ramp are measured to determine the metering rate.
- Closed-Loop Local Control Strategies: For closed-loop control, system output is fed back and the input is modified with respect to the output. Here the aim is to set the output value at a desired level. In this study linearized local-feedback control algorithm ALINEA is used which will be explained in Section 5.3.1. There are also other closed-loop local control strategies such as fuzzy logic control [40].

#### **3.2.1.2 Systemwide (Coordinated) ramp metering control strategies**

Systemwide ramp metering is a control system which considers a network with various sequential or coordinated ramps. Improving traffic flow at a highway intersection may not be sufficient for a relaxation in a whole network. It may also be harmful to the other consecutive segments. That is why the whole network should be under consideration while optimizing the traffic flow. For that purpose

systemwide (coordinated) ramp metering control strategies are taken into account. Examples of systemwide ramp metering control strategies are FLOW [41], Zone (Minnesota) algorithm [42], Stratified Zone (new Minnesota) algorithm [43], Helper [44], METALINE [45] and SWARM [46].

### 3.2.2 Variable speed limit

The ideal VSL system consists of sensors, variable speed limit signs, variable message signs, and a central processing unit to execute control actions. As shown in Figure 3.1, VMS are used to inform drivers of the traffic condition ahead and to display the enforced speed limit based on the VSL control strategies.



**Figure 3.1:** VSL Control in Istanbul [8]

Depending on the approaching volume, driver compliance rate, and the resulting congestion, the central processing unit that integrates all system sensors and signs will compute the time-varying optimal speed limit for each VMS dynamically and display it in a timely fashion [47].

Common practice over the past several decades for work zone operations is to recommend or enforce a reduced speed limit via variable message signs (VMS), which may or may not respond to fluctuations in approaching traffic demand. To properly respond to traffic conditions and to increase the compliance rate of drivers, traffic professionals in recent years have experimented with variable speed limit (VSL) control in place of the conventional posted speed limit operations in highway work zones [47].

In brief, most existing VSL-related systems have been designed in response to traffic safety concerns but not for improving operational efficiency, such as to maximize the throughput from a work zone segment or to minimize the average delay for vehicles traveling through the entire highway segment plagued by the work zone-imposed traffic queue. Our study intends to address this critical issue with a dynamic VSL control algorithm for highway work zone operations. Our proposed VSL system dynamically adjusts the set of displayed optimal speed limits based on the detected occupancies at the bottleneck section of the freeway, so as to effectively respond to potential demand variation and establish a smoother flow along the stretch.

### 3.2.3 Lane closure and allocation

For controlling the traffic flow, lane closure is made by traffic regulators. Here the main purpose is to increase or decrease the capacity by allocating or closing one or more lanes. In Turkey, a lane allocation is made at Boğaziçi Bridge which can be seen in Figure 3.2.



**Figure 3.2:** Lane Allocation in Istanbul [9]

There are also some worldwide examples in [48].





## **4. TRAFFIC SIMULATION**

Whatever the branch of engineering is, all engineers are investigating on various systems that they concern. A system is a set of its components, which exists and operates in time and space. In order to understand the structure of the investigated system, engineers make field observations and according to that observations they establish models. Simulation is a way to execute the modelled processes, which aims to demonstrate or to solve the real world problems of engineering.

Simulation plays an important role in traffic engineering and planning. Traffic simulation is considered by three main classifications of traffic models. First, the classification is made according to the given input. If traffic is invariant over time, this type simulations models the steady-state average traffic conditions and is stated as static; if traffic changes over time, this type models the variant nature of traffic and is stated as dynamic.

Another classification of traffic models is defined as their statistical point of view. If the outputs of the traffic simulations are different by their executions, i.e. if there is a randomness at the modelling process it is called stochastic modelling of traffic. If the simulations demonstrates the same output in every execution, it is called deterministic modelling of traffic.

The last and the most important classification of traffic is the level of detail classification of traffic flow, which will be explained in this section.

### **4.1 Macroscopic Simulation**

All the traffic models described in Section 2 are considered as macroscopic modelling. As it is first proposed, the first macroscopic model of traffic flow LWR Model used the analogy between traffic flows and fluid flows. It is based on two assumptions that no cars disappear or appear suddenly on a conservative road. Later various models analog

to the gas dynamics and representing multiregimes are proposed. The simulations based on these theories are called macroscopic simulation. In these simulations level of detail is limited and the traffic parameters are roughly considered, so the need of discretization of time and space is emerged [22] [23].

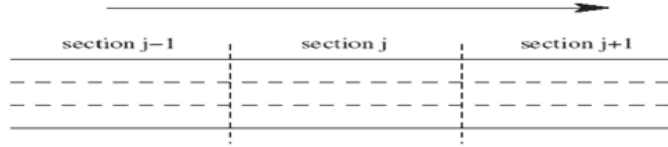


**Figure 4.1:** Discrete Highway Sections [10].

## 4.2 Microscopic Simulation

As used in this study, the state-of-art simulation programs are based on microscopic traffic flow models. Microscopic traffic flow models concern individual car movements rather than averaged variables used as in macroscopic traffic flow models.

It should be underlined to prevent the misunderstandings about this study that a microscopic simulation environment is used to test control algorithms based macroscopic theories of traffic flow. The reason why the control algorithms are based on macroscopic theories is the field applications of the control algorithms are in macroscale, because there is no way to control individual vehicles for today.

Here the most known microscopic traffic model is the linear car-following model. It is based on the elementary Newtonian physics law theory which is response is equal to the stimulus. However in reality, there is a sensitivity constant between response and stimulus which makes the "equal" word in that theoretical proposition "proportional" [49]. All the things said above is nothing but

$$response = sensitivity \times stimulus. \quad (4.1)$$

In car-following model the fundamental principle is as in Equation (4.1). Let us consider a line of cars moving on a road as in Figure 4.2.

In car-following model the stimulus action is defined as the change at the speed difference between the leader denoted as  $n$ th car and the follower denoted as  $(n + 1)^{st}$  car. On the other hand, response is modeled as the acceleration of the follower car after

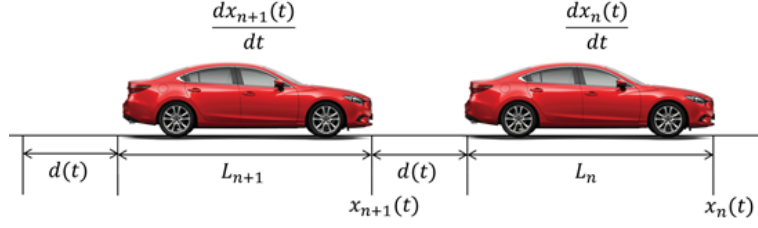


**Figure 4.2:** Line of Cars Moving on a Road.

a reaction time  $T$  which is denoted as the  $(n+1)^{st}$  car. So Equation (4.1) yields

$$\frac{d^2 x_{n+1}(t+T)}{dt^2} = -C_1 \left( \frac{dx_{n+1}(t)}{dt} - \frac{dx_n(t)}{dt} \right) \quad (4.2)$$

where  $-C_1$  denotes the sensitivity. By integrating Equation (4.2)

$$\frac{dx_{n+1}(t+T)}{dt} = -C_1(x_{n+1}(t) - x_n(t)) \quad (4.3)$$

where  $C_2$  is an arbitrary constant. From Figure 4.2 the spacing may be seen as

$$d(t) = x_n(t) - L_n - x_{n+1}(t) \quad (4.4)$$

where  $L_n$  is the length of the  $n^{th}$  car. Let us consider a road segment from the start of the spacing between  $(n+2)^{nd}$  and  $(n+1)^{st}$  cars till the end of the car  $n$  which is  $x_{n+1}(t)$ . The density will be from Equation (2.1)

$$\rho = \frac{2}{L_n + L_{n+1} + 2d(t)}.$$

Assuming  $L_n \rightarrow L_{n+1}$  and using Equation (4.4) yields

$$\rho = \frac{1}{L_n + d(t)} = \frac{1}{x_n(t) - x_{n+1}(t)}. \quad (4.5)$$

If this result will be plugged into Equation (4.3)

$$u(\rho) = \frac{dx_{n+1}(t+T)}{dt} = \frac{C_1}{\rho} + C_2 = C_1 \left( \frac{1}{\rho} + \frac{C_2}{C_1} \right). \quad (4.6)$$

Here  $-C_2/C_1$  is the cutting point of the  $x$ -axis so it will be denoted as  $\rho_{jam}$ . This macroscopic variable representation of the car-following model is represented in Figure 4.3.

As it can be seen in Figure 4.3,  $u \rightarrow \infty$  where  $\rho \rightarrow 0$ . So there should be an upper bound for speed after a critical density say  $\rho_c$  in order to meet the empirical results. So

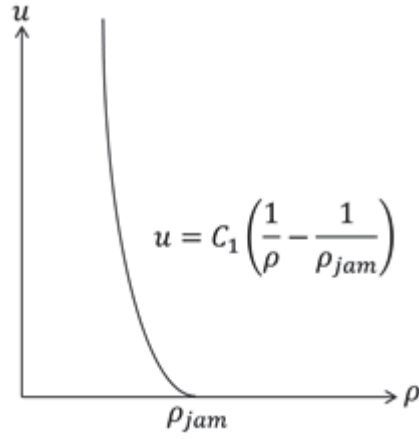


**Figure 4.3:** A Curve for Illustrating Speed-Density Relationship proposed from Car-Following Model.

this result yields to a piecewise function

$$u(\rho) = \begin{cases} u_f & , \rho < \rho_c \\ C_1 \left( \frac{1}{\rho} - \frac{1}{\rho_{jam}} \right) & , \rho \geq \rho_c \end{cases} \quad (4.7)$$

Flow-density relationship also can be found by applying Equation (2.5)

$$q(\rho) = \begin{cases} \rho u_f & , \rho < \rho_c \\ C_1 \left( 1 - \frac{\rho}{\rho_{jam}} \right) & , \rho \geq \rho_c \end{cases} \quad (4.8)$$

In Figure 4.4 the bilateral relationships density-speed density-flow are represented.

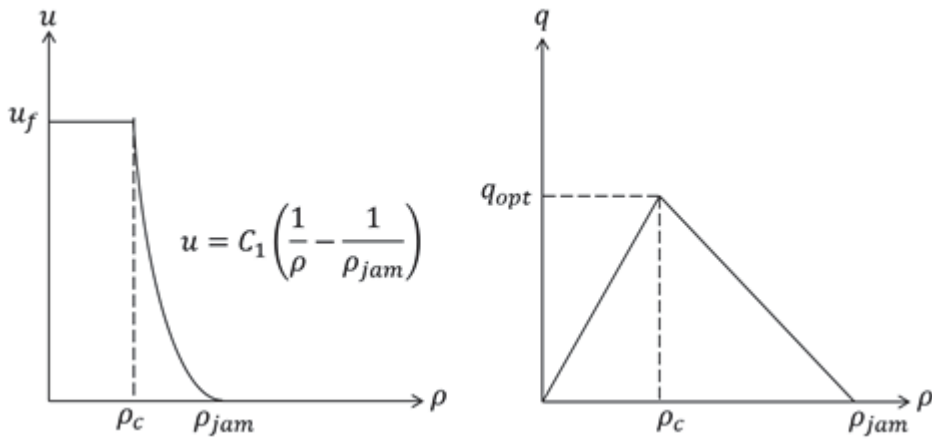


**Figure 4.4:** Density-Speed and Density-Flow Relationships proposed from Car-Following Model.

### 4.3 Mesoscopic Simulation

In mesoscopic simulation, individual modelling of vehicles are concerned, but in contrary to the microscopic simulation, aggregate behaviour of the vehicles are considered on links. Cell automata is a mesoscopic model for mesoscopic simulation of traffic flow. It is based on the propagation of the vehicles through cells, which is illustrated in Figure 4.5.

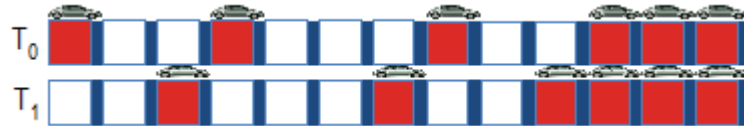


**Figure 4.5:** Vehicle Propagation based on Cell Automata Traffic Flow Model [10].

Another example for mesoscopic model is event based mesoscopic model Mezzo. Macroscopic modeling concept of shock waves and microscopic modeling concept of route assignment is also valid for this model [10].

As a brief illustration of these concepts of simulation types are demonstrated in Figure 4.6.

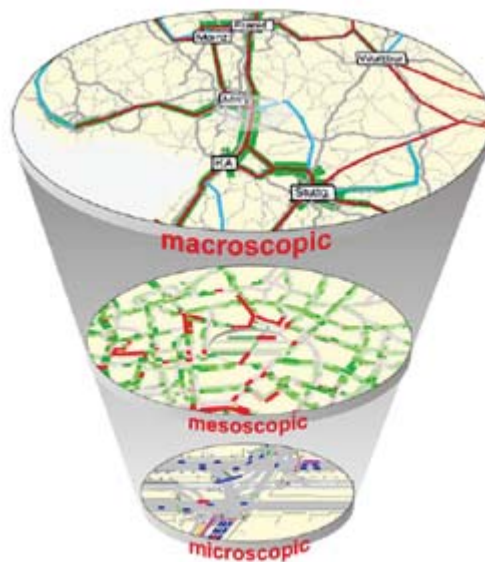


**Figure 4.6:** Macro-Meso-Microscopic Simulation Comparison [11].



## **5. DYNAMIC FREEWAY TRAFFIC FLOW CONTROL APPROACHES IN MICROSCOPIC TRAFFIC SIMULATOR PTV VISSIM**

In this section, two main dynamic traffic flow control approaches are introduced and applied. Firstly, the study field is described. Then the microscopic simulation environment PTV VISSIM is introduced and the calibration process is explained. Finally, the two main dynamic traffic flow control approaches, which are dynamic ramp metering and variable speed limit control approaches are expressed and the application results of these approaches are discussed.

### **5.1 Study Field**

As study field Levent Ramp of Istanbul Outer Beltway (O-2) is determined. A satellite quicklook image of the study field is presented in Figure 5.1 and a rough illustration of the study field.

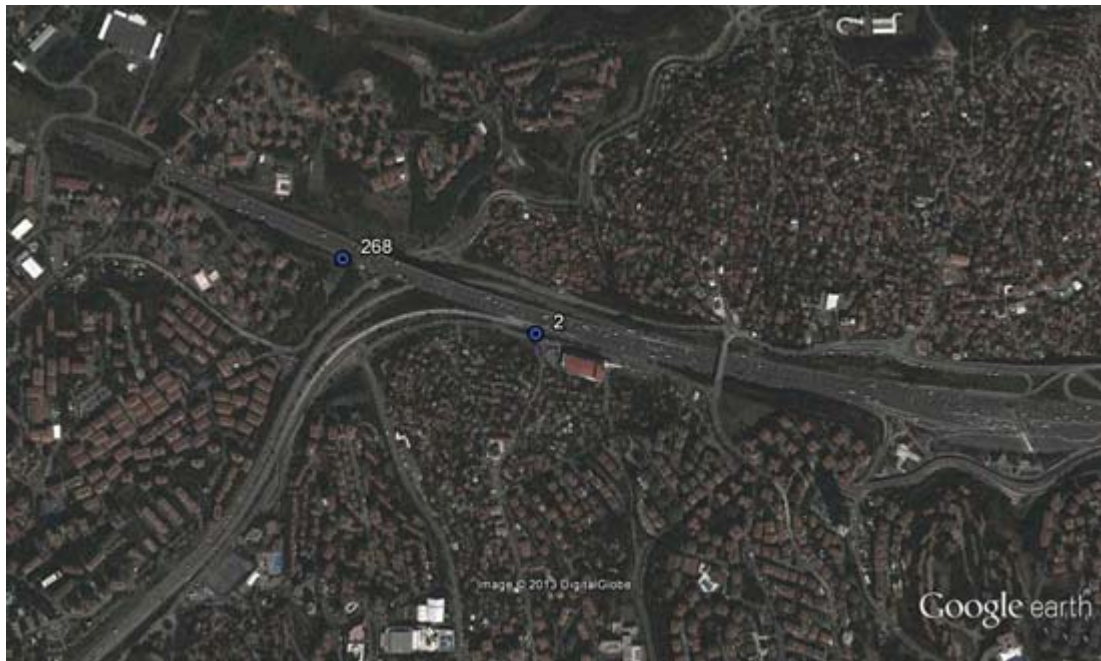


**Figure 5.1:** Satellite Quicklook Image of the Study Field (Google Earth®).

RTMS (Remote Traffic Microwave Sensor) is a sensor used to collect the data from the section of the highway on which RTMS is set up. Occupancy rate, long and all vehicle volume and speed data were collected on daily, time and lane basis with RTMS. Here, there is a need of a basic definition of occupancy rate.

Occupancy time is the time in seconds that how many seconds do the detector or sensor is occupied by the vehicles. The ratio between the occupancy time of the detector and the measurement interval gives the occupancy rate, which can also be said temporal concentration [25] or relative density.

The data were collected at the RTMS Point 2 as it can be seen in Figure 5.1 between the days 06.07.2010 (Tuesday)-13.07.2010 (Tuesday) which does all includes regular days (non-holidays, regular weather conditions, etc.) with the non-uniform time difference between the two consequent RTMS measurements varies between 42-240 seconds but mostly 120 second. The time difference histogram of the RTMS measurements is presented in Figure 5.2.

Since the data are mainly 2 minute data, a data refining policy is taken into account. For flow<sup>1</sup>, 8 sequential time interval volume data are aggregated and scaled into 60 minutes in order to find the flow rate, which will be given as parameters to the simulation program. Speed data are averaged as weighted arithmetic averages of 8 consecutive speed measurements with respect to the flow of each time interval. Occupancy rates are also calculated as weighted arithmetic averages of 8 consecutive occupancy rate measurements with respect to the time difference of each time interval. The flow data are represented in Figure 5.3.

Here in Figure 5.3, it can be seen that each day is more or less identical to each other. For vehicle input scenario 08.07.2010 (Thursday) 14:45:28-23:48:56 is selected where afternoon peak, low inflow, moderate inflow and high inflow for both main stream and ramp are seen. Flow data for the whole day 08.07.2010, for the selected hours and HGV composition change are shown in Figure 5.4 and 5.5 respectively.

---

<sup>1</sup>Here flow denotes flow rate.



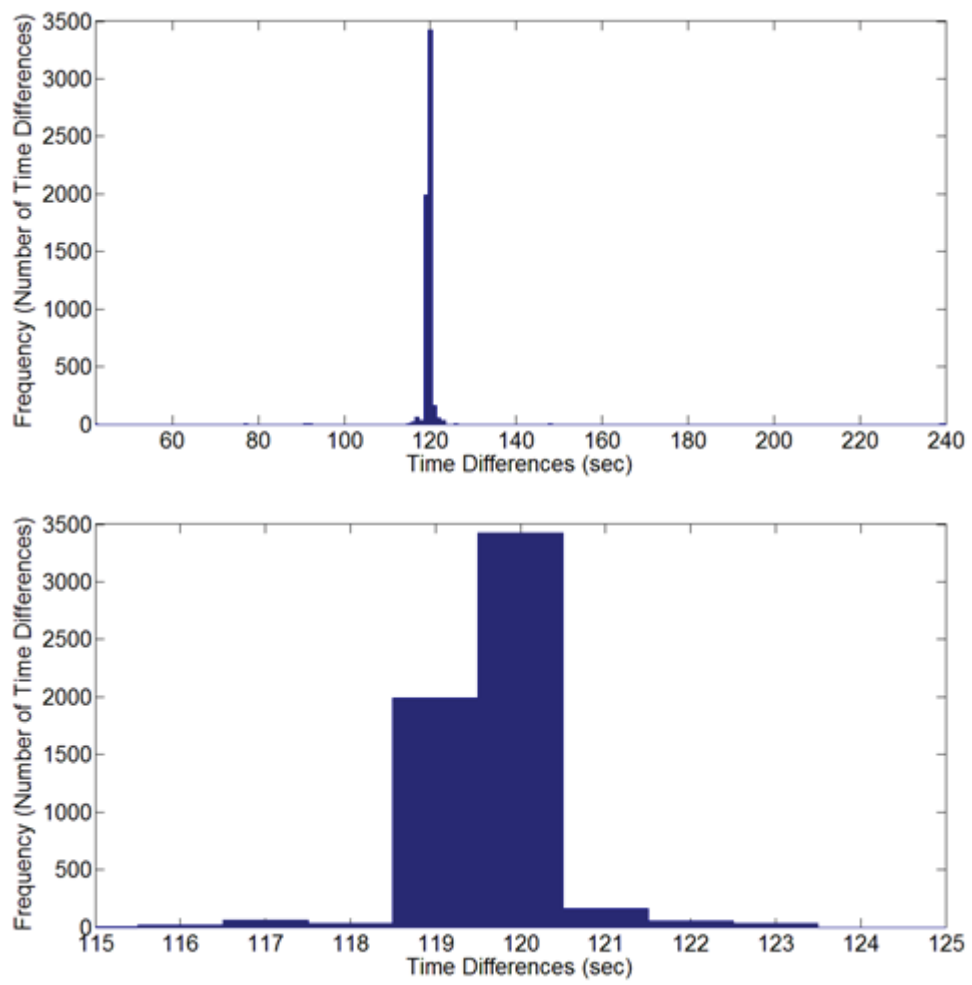


**Figure 5.2:** Histogram for the Time Difference Data.

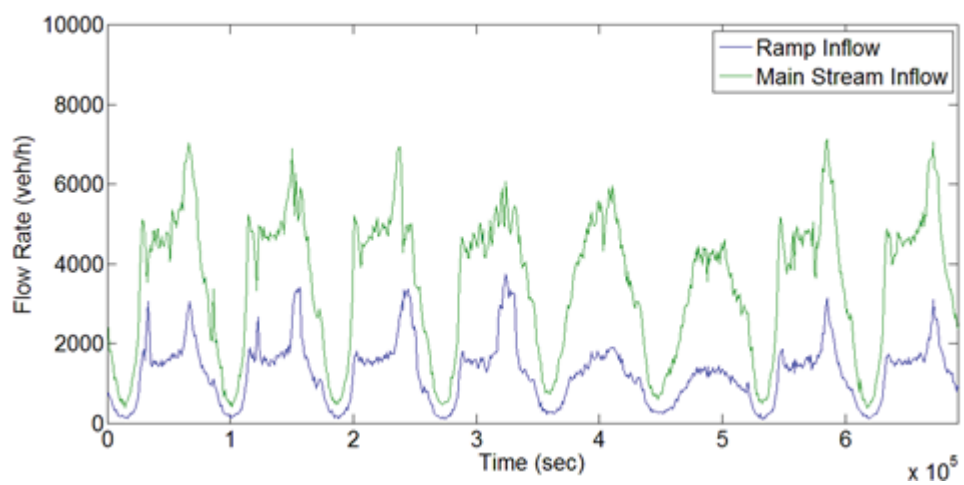


**Figure 5.3:** Flow Data for 8 Days.

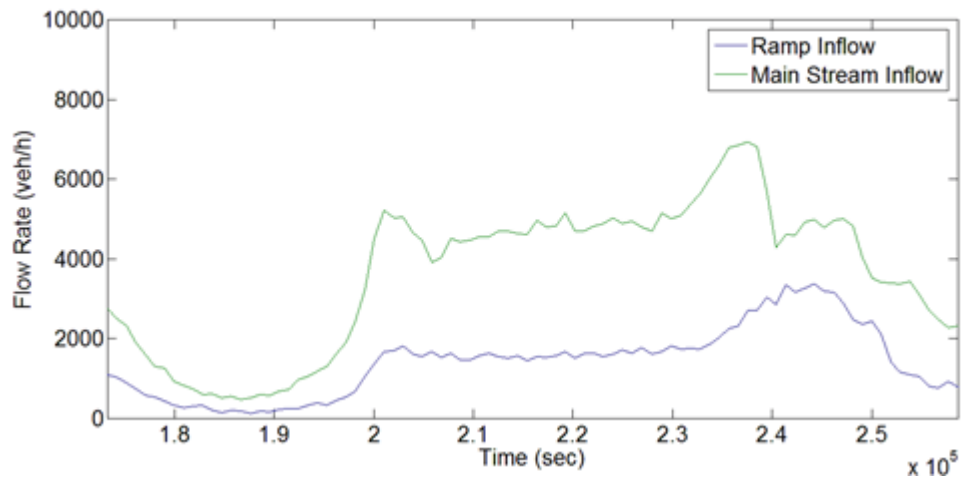


**Figure 5.4:** Flow Data for 08.07.2010 (Thursday).

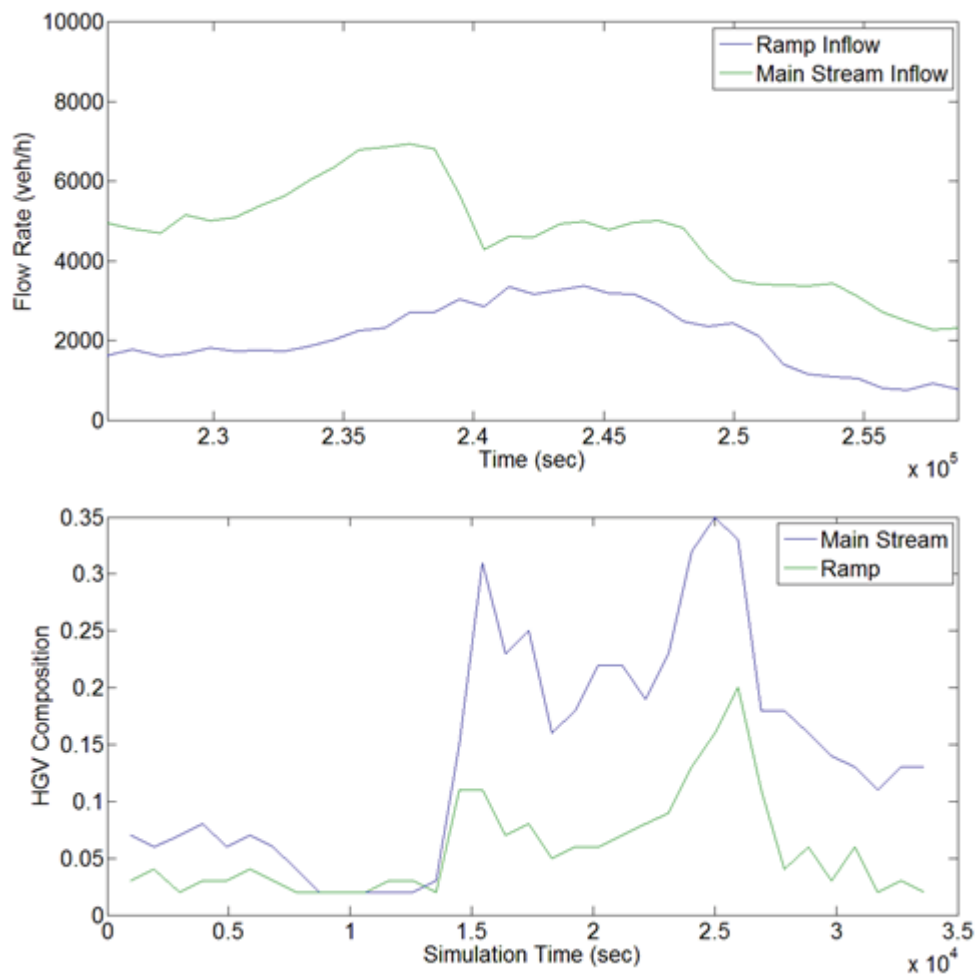


**Figure 5.5:** Flow Data (Up) HGV Composition for 08.07.2010 (Thursday)  
14:45:28-23:48:56 (Down)

## **5.2 Microscopic Simulation Environment PTV VISSIM**

PTV VISSIM is a microscopic simulation program based on the driving behavior model of Wiedemann proposed in 1974 [50] and in 1999 [51]. PTV VISSIM is developed by PTV AG (Planung Transport Verkehr Aktiengesellschaft) and written in C++ considering guidelines of object oriented programming (OOP) [52].

PTV VISSIM not only enables to monitor actual state of traffic and but also enables to simulate and evaluate the macroscopic traffic variables as in real life. In many cases the precautions, suggestions or changes are done with regard to the simulation results. PTV VISSIM is also able to demonstrate the multimodal structure of the area such as public transit busses, heavy rail or pedestrians which is defined by the user. There are two main driving behavior which is logically based on longitudinal and lateral movements, since all the movements on the road surface can be represented as a superposition of those two main movements.

### **5.2.1 Longitudinal movement model: Wiedemann Car Following Models**

Wiedemann's Car Following Models used for longitudinal movements in PTV VISSIM simulation program are mainly based on the psychophysical driving behavior of the drivers. In [12] four main phases of driving is defined:

- **Free Driving:** If there is no observable car in front, the drivers tend to keep their desired speeds. In reality, since the driver behavior is not perfect the drivers cannot keep their speeds constant but their speeds oscillates with respect to time.
- **Approaching:** In this phase, the driver observes a preceding driver, which propagates slower in the front and decelerates as he/she keeps the desired safety distance.
- **Following:** The driver tends to keep the safety distance but regard to his/her imperfect driving behavior his/her velocity oscillates.
- **Braking:** This happens when the distance goes down to the safety distance due to a sudden decrease of the speed of the preceding vehicle or an another vehicle

suddenly changes the lane and becomes the preceder of that vehicle. This is called platooning or shock wave effect in traffic engineering literature when it happens sequentially.

These states are represented in Figure 5.6.

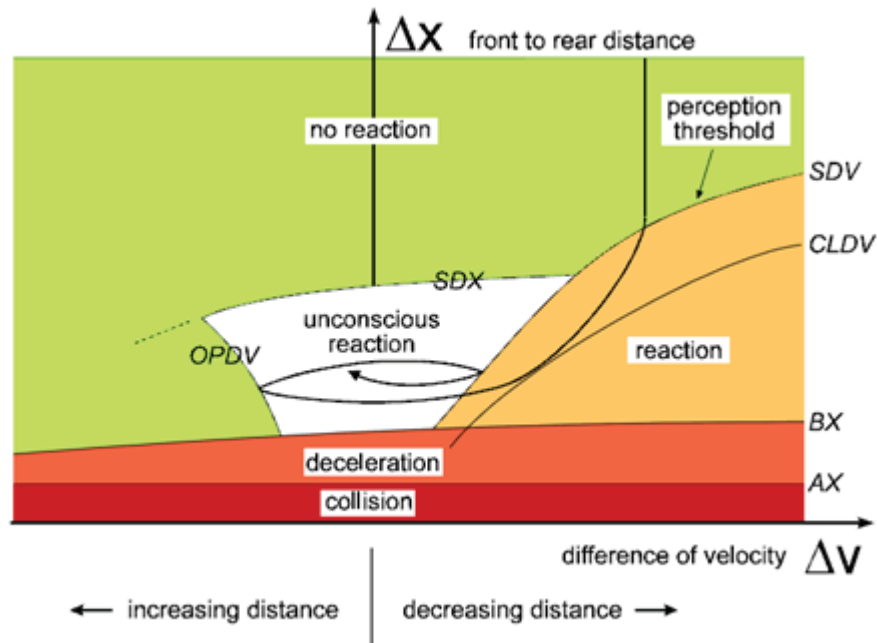


**Figure 5.6:** Wiedemann's Car Following Model [12].

### 5.2.2 Lateral movement model

Lateral movements are mainly considered in lane changing movements in PTV VISSIM. There are two main lane change types considered which are lane changing from the fast lane to the slow lane and from the slow lane to the fast lane which are highly considered in [12].

### 5.2.3 Network elements

In PTV VISSIM, the entire roadway infrastructure is represented with specific network elements. Here are some of which are used for this study.

- **Links and Connectors:** Roads are represented as links and two preceding link is connected with a connector in PTV VISSIM.

- **Desired Speed Decisions:** When a car passes this sign its desired speed is adjusted according to the given desired speed.
- **Signal Head:** The signal head is used as it is in the field. When the signal head turns red, cars will stop and when it turns green, cars will go. This element can be either controlled fixed time or by a VAP code.
- **Detectors:** Detectors are devices to observe vehicles and people. It can return occupancy rate, number of vehicles passed, headway, occupancy time, vehicle length, velocity, etc.
- **Reduced Speed Areas:** The vehicles adjust their desired speeds when they enter that area and change their desired speeds to normal thereafter.
- **Data Collection Points:** This is used for evaluating the performance of the specified section. Number of vehicles passed, occupancy rate, persons, queue delay time, mean and average speed are some parameters which users can obtain from data collection points

#### 5.2.4 Calibration and verification

Various approaches for calibration of VISSIM are made by various scholars. For example, GEH index [53] is proposed for calibration which can be calculated as

$$GEH = \sqrt{(2(Q_o - Q_s)^2)/(Q_o + Q_s)} \quad (5.1)$$

where  $Q_o$  denotes observed and  $Q_s$  denotes simulated volumes. In this case GEH index is not valid, since the time differences between the two consequent RTMS measurements are not uniform with respect to time.

An another approach for simulation calibration process is made by adjusting the driving behaviour parameters of Wiedemann 74 and 99 models [54]. Since the scope of this study is not calibration and there is no microscopic data available, this calibration process can not be made.

In this study, speed-volume diagram is plotted for calibration in order to check and validate the accuracy of the speed-volume diagram between the simulation results and

field observations as it proposed in [52]. These diagrams are very useful for calibration because they contain information about a broad range of traffic situations. In particular they show how the traffic flow behaves around capacity. This is the reason why these speed–flow diagrams are often used for comparing simulation results with real-world data. An another purpose for looking at the speed-volume scatter plots is to see whether the desired volumes can pass through an intersection with the desired speeds or not. It is found that the simulation is valid and accurate by looking at the speed-volume diagram. The results are presented in Figure 5.7, 5.8 and 5.9.

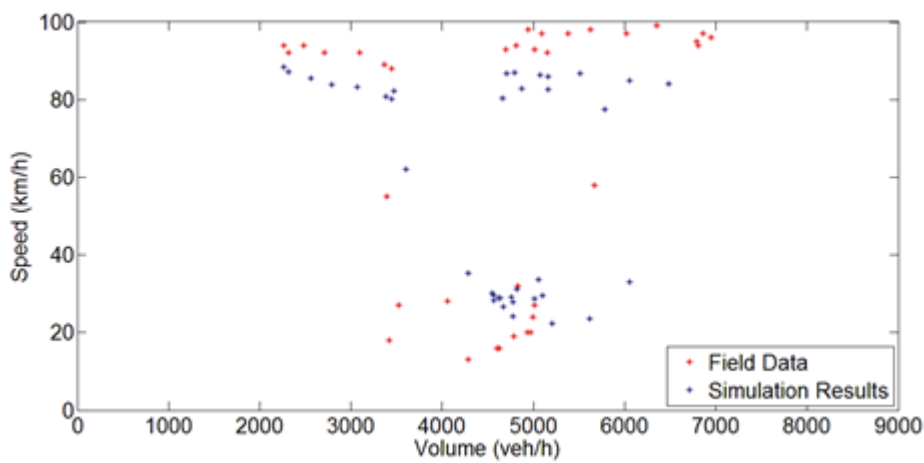


**Figure 5.7:** Speed-Flow Calibration/Verification Results for Main Stream

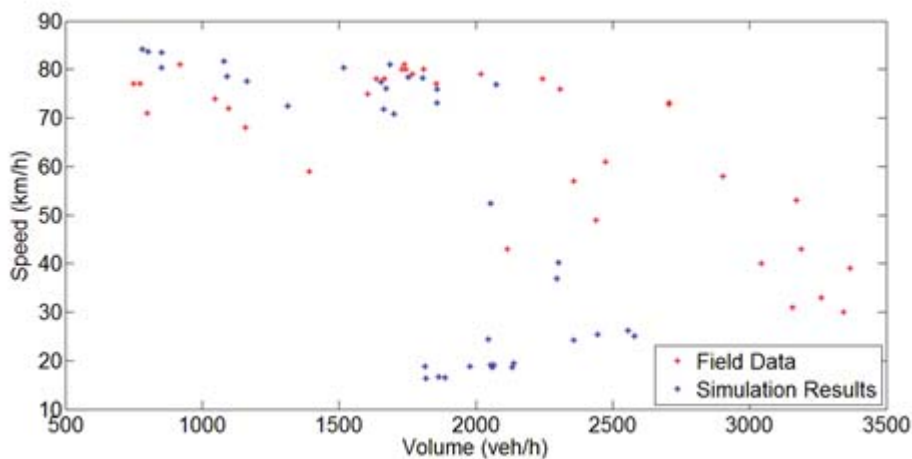


**Figure 5.8:** Speed-Flow Calibration/Verification Results for Ramp

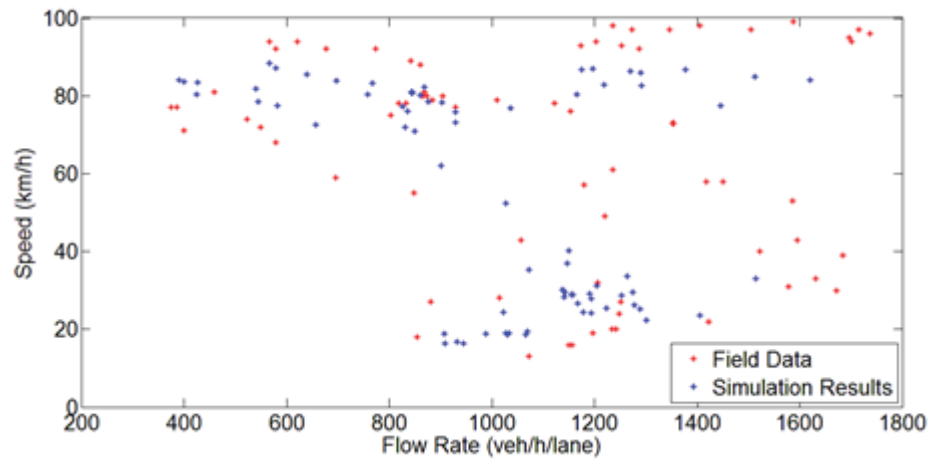


**Figure 5.9:** Speed-Flow Calibration/Verification Results for Whole Section

### 5.3 Dynamic Traffic Flow Control Approaches in PTV VISSIM

For the study field and data described in Section 5.1, the network is generated, the vehicle inputs (traffic volumes and vehicle composition) are entered as it proposed in Section 5.1 and calibration is made as it is explained in Section 5.2.4. Simulation interface is shown in Figure 5.10.

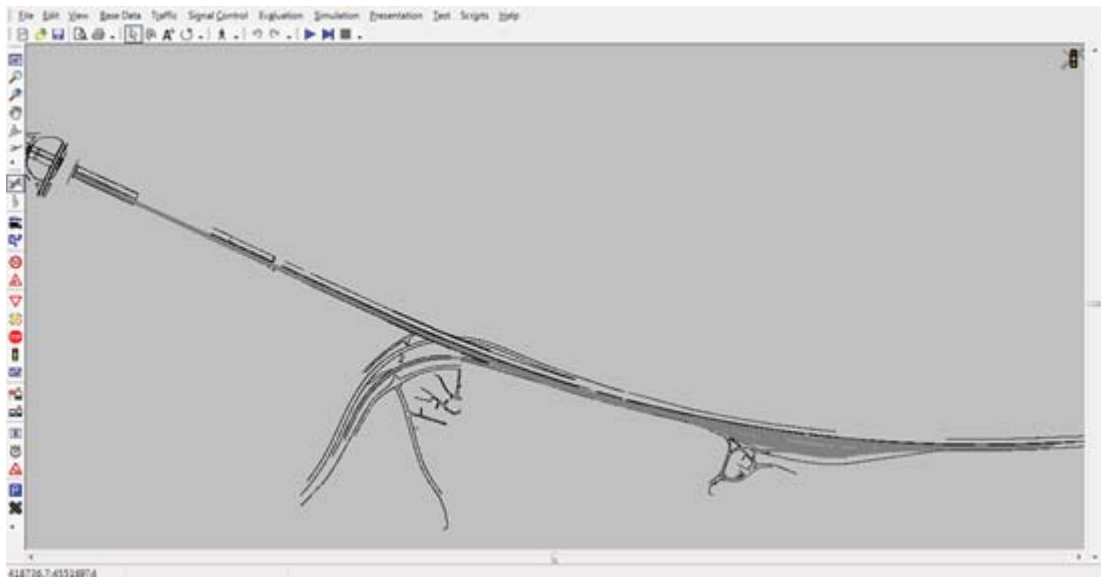


**Figure 5.10:** Study Network generated in PTV VISSIM.

For the evaluation process in order to use in dynamic traffic flow control approaches data collection points are positioned at the 50<sup>th</sup> meter of the downstream link as it proposed in [38] which is shown in Figure 5.11.

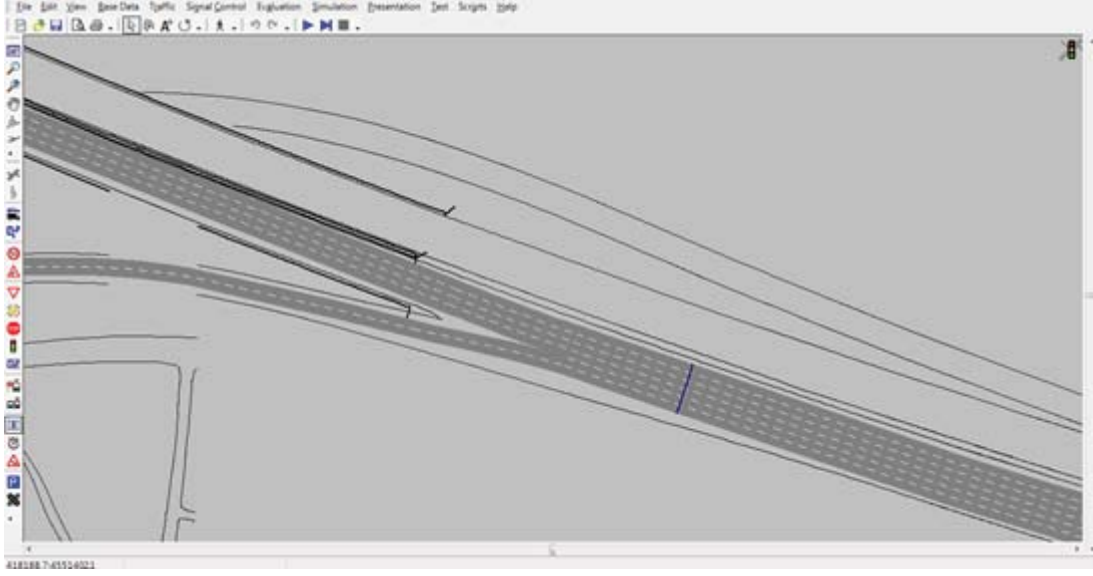


**Figure 5.11:** Data Collection Point Locations.

Occupancy rates are measured with a time interval 20 sec since one of the ramp metering approach and all the variable speed limit approaches have the cycle time 20 sec. For the obtained results a regression model is proposed in order to predict the traffic and take precautions. The regression model is

$$o(t + \Delta t) = c_0 o(t) + c_1 o(t - \Delta t) + c_2 o(t - 2\Delta t) \quad (5.2)$$

where  $o(t + \Delta t)$  is the next occupancy rate rate which is predicted to be measured in the next cycle,  $o(t)$  is the current occupancy rate which is measured in the same time interval,  $o(t - \Delta t)$ ,  $o(t - 2\Delta t)$  and  $o(t - 3\Delta t)$  are the occupancy rates which have been measured in the past first, second and third time intervals respectively and  $c_i$ 's are normalized constants to be determined. After the regression analysis  $c_0 = 0.29$ ,  $c_1 = 0.02$  and  $c_2 = 0.69$  are taken. The results of regression analysis is given in Table 5.1 and the occupancy rate prediction model is shown in Figure 5.12.



**Table 5.1:** The Results of Regression Analysis.

Regression Statistics	
Multiple R	0.98
R Square	0.95
Adjusted R Square	0.95
Standard Error	0.95
Observations	798

ANOVA	df	SS	MS	F	Significance F
Regression	2.00	86.85	43.43	8001.64	0.00
Residual	796.00	4.32	0.01		
Total	798.00	91.17			

	Coefficients	Standard Error	t Stat	P-value	Lower 95 %	Upper 95 %
$o(t)$	0.29	0.03	11.34	0.00	0.24	0.35
$o(t)$	0.02	0.10	56.71	0.00	0.73	0.69
$o(t)$	0.69	0.03	26.52	0.00	0.64	0.74

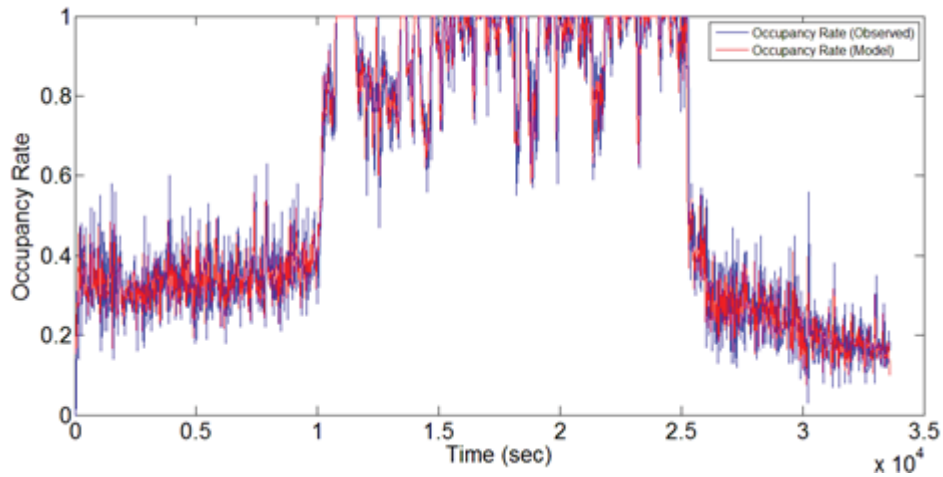


**Figure 5.12:** Occupancy Rate Prediction Model.

Downstream link is segmented into 50 meter multiple segments and from the link evaluation option density is collected in order to plot density profile along the downstream link. The result is demonstrated in Figure 5.13.

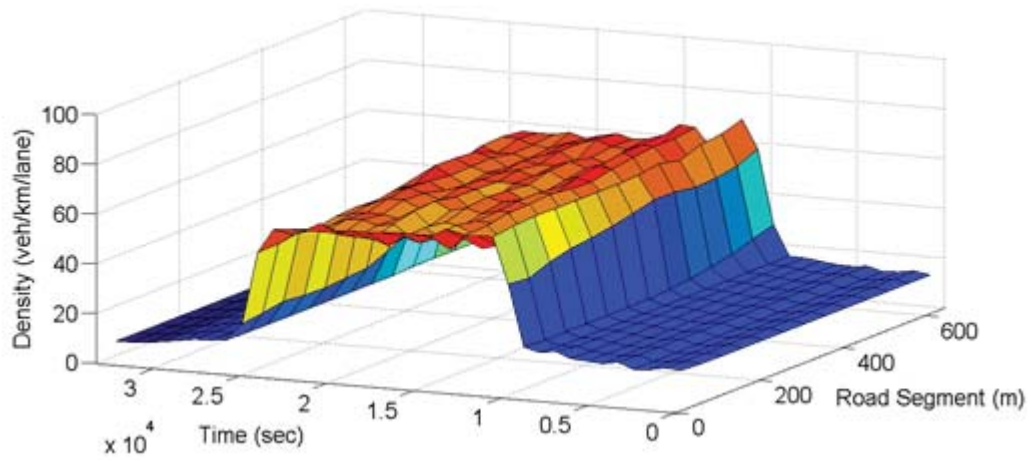


**Figure 5.13:** No Control Density Profile.

### 5.3.1 Ramp metering approach

For this approach, ALINEA (Asservissement Lineaire d'Entree Autoroutiere-French for "Linear Utilization for Highway Entrances") ramp metering strategy proposed by Papageorgiou, M., Hadj- Salem, H. and Blosseville, J. M. in 1991 [19]. This strategy aims to keep the occupancy rate at a level of desired occupancy rate which is generally

taken 0.30 as it proposed by their authors. The main step of this strategy is given as

$$r(t + \Delta t) = r(t) + K_r(\hat{o} - o(t + \Delta t)) \quad (5.3)$$

where  $r(t + \Delta t)$  is called the metering rate to release to the downstream at the next cycle,  $r(t)$  is the metering rate which is released at the current cycle,  $K_r$  is a regulator parameter which is taken generally 70 by the authors and the applicators of this algorithm,  $\hat{o}$  is the desired occupancy rate and  $o(t + \Delta t)$  is the predicted occupancy for the next cycle.

In order to apply this to the VAP module for PTV VISSIM, in simulation 5 meter detector is placed at the 50th meter of the downstream as the data collection point location in no control case. This is shown in Figure 5.14.

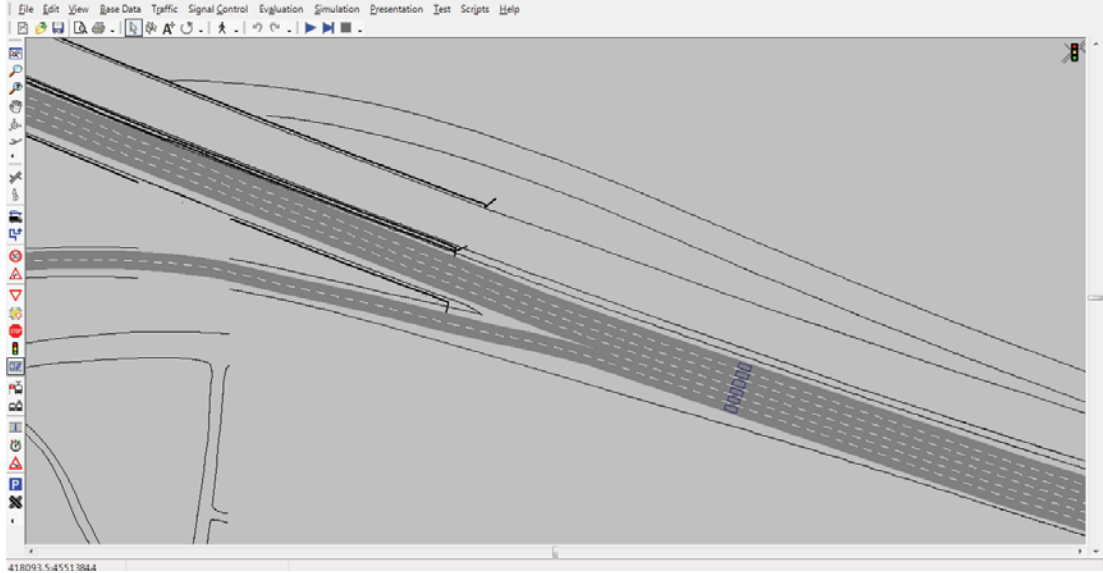


**Figure 5.14:** Detector Locations.

As it proposed in [38], signal heads are placed 130 meter upstream of the ramp. This is pictured in Fig5.15.

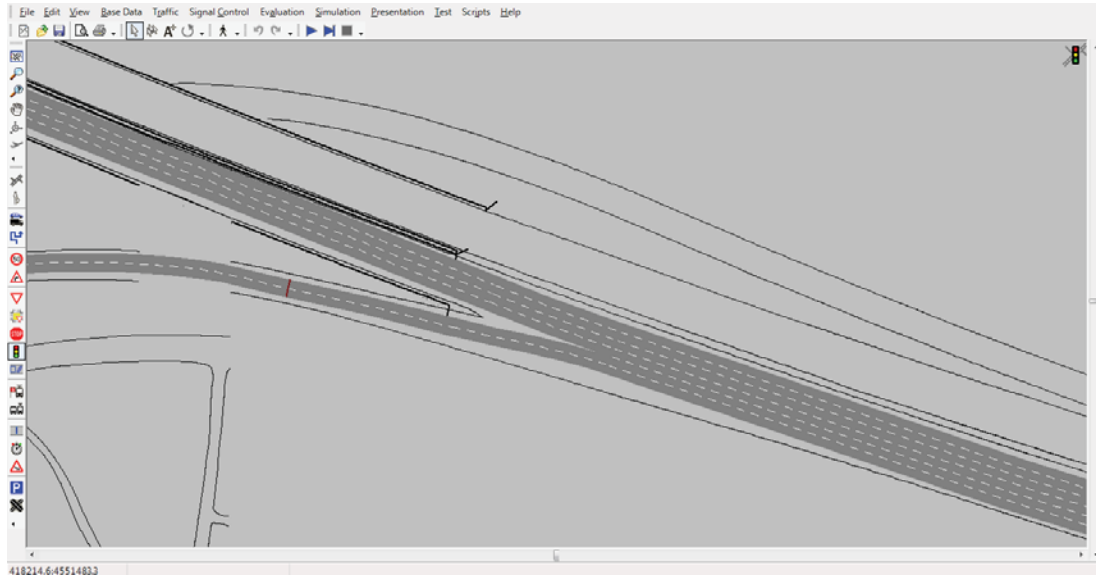


**Figure 5.15:** Signal Head Locations.

In this study two applications for ALINEA approach are coded in VAP. In the first approach, cycle time  $\Delta t$  is taken as 20 sec and the minimum green time is taken as 10 sec. The green time fluctuation with respect to occupancy rate measured is demonstrated in Figure 5.16.

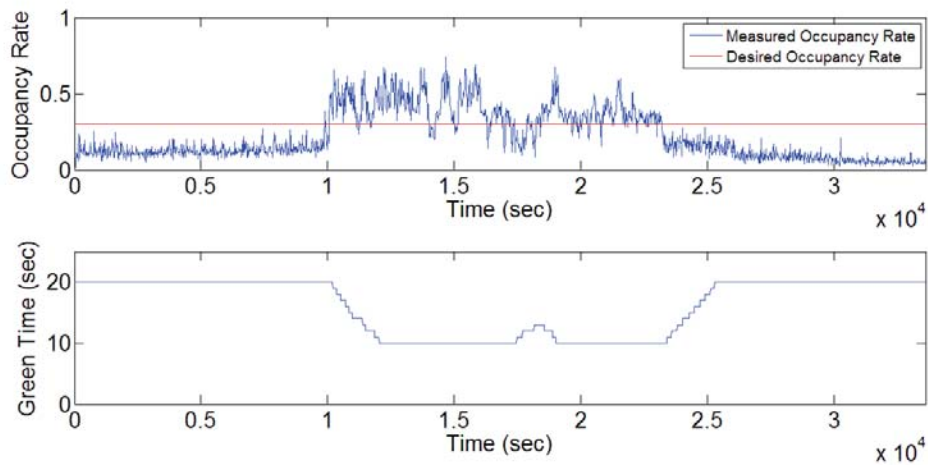


**Figure 5.16:** Green Time Fluctuation with Respect to Occupancy Rate Measured for Ramp Metering Approach 1 (Cycle Time=20 sec, Minimum Green Time=10 sec).

The density profile for the first approach is demonstrated in Figure 5.17.

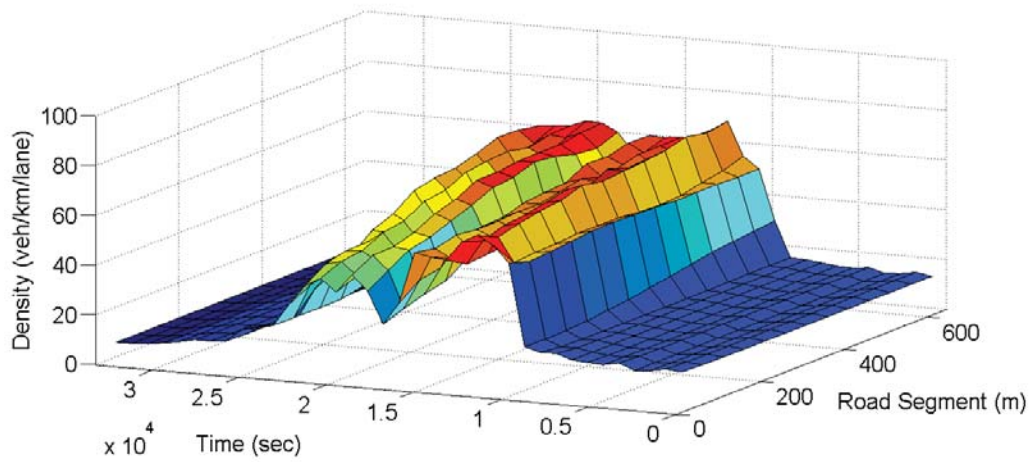


**Figure 5.17:** Density Profile for Ramp Metering Approach 1 (Cycle Time=20 sec, Minimum Green Time=10 sec).

In the second approach, cycle time  $\Delta t$  is taken as 15 sec and the minimum green time is taken as 5 sec. The green time fluctuation with respect to occupancy rate measured is demonstrated in Figure 5.18.

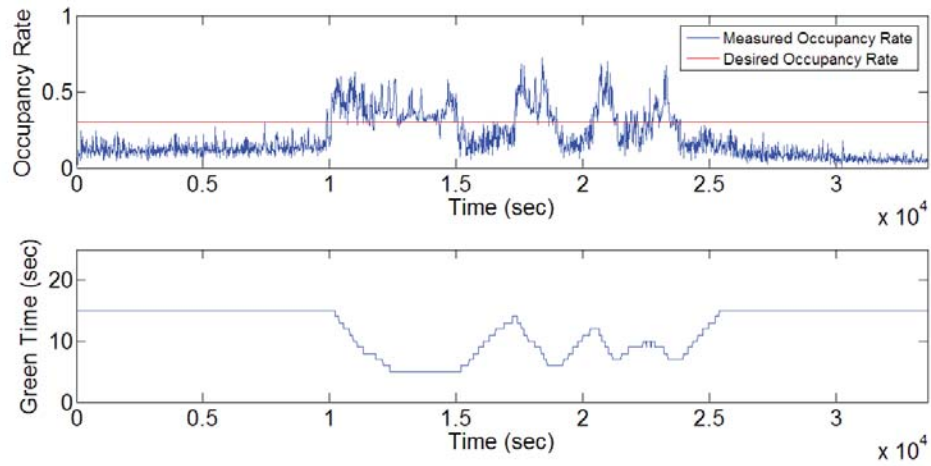


**Figure 5.18:** Green Time Fluctuation with Respect to Occupancy Rate Measured for Ramp Metering Approach 2 (Cycle Time=15 sec, Minimum Green Time=5 sec).

The density profile for the second approach demonstrated in Figure 5.19.

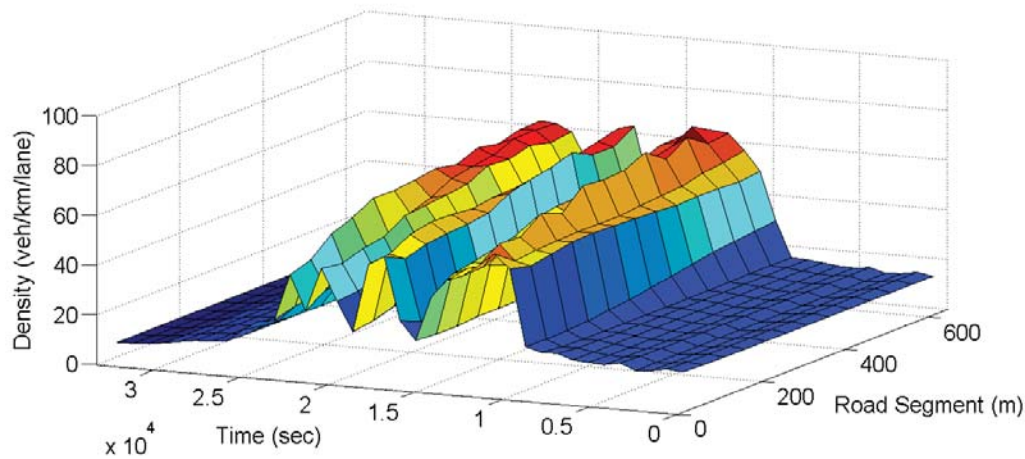


**Figure 5.19:** Green Time Fluctuation with Respect to Occupancy Rate Measured for Ramp Metering Approach 2 (Cycle Time=15 sec, Minimum Green Time=5 sec).

The optimal cycle time or minimum green time is also a problem for ramp metering approaches but this problem is not in the scope of this study. There are various studies for that problem. For example, in [38] it is taken 2 seconds or in [55] it is examined 10 to 300 seconds. However in this study, more applicable cycle time policy to the field such as 15 and 20 seconds are considered since the drivers may be confused if cycle time is selected too short, although it may be give better results in theory.

### 5.3.2 Variable speed limit approach

For this approach, desired speed decisions for main stream and ramp are placed 1300 meter upstream of main stream and 400 meter upstream of ramp which is demonstrated in Figure 5.20.

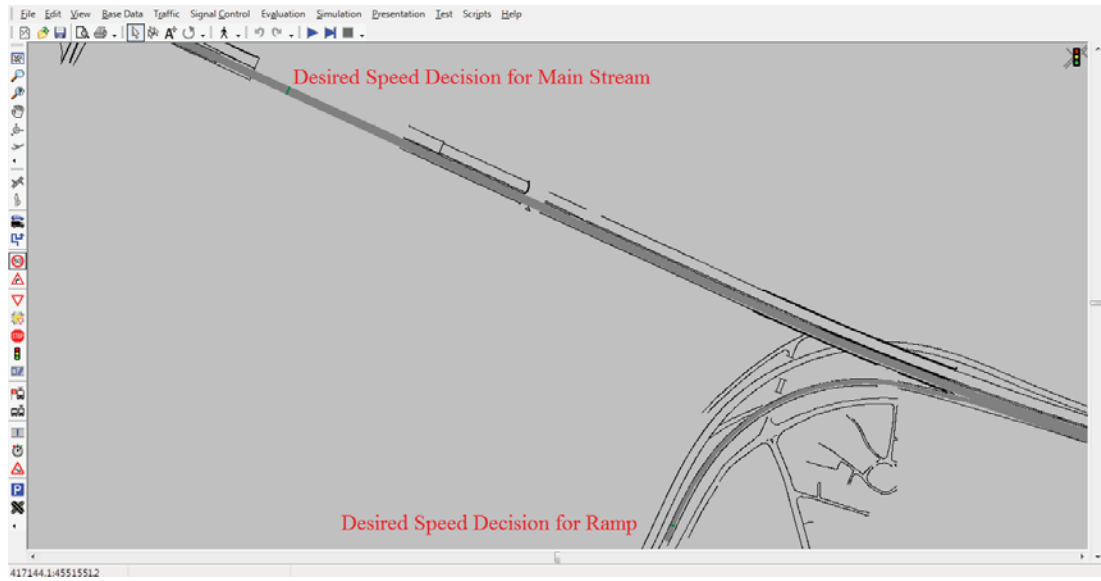


**Figure 5.20:** Desired Speed Decision Locations for Main Stream and Ramp.

Nearly at the end of the network desired speed decisions also placed in order to discharge the traffic and assigned 90 km/h and 60 km/h desired speed decisions for cars and heavy good vehicles respectively. This is shown in Figure 5.21.

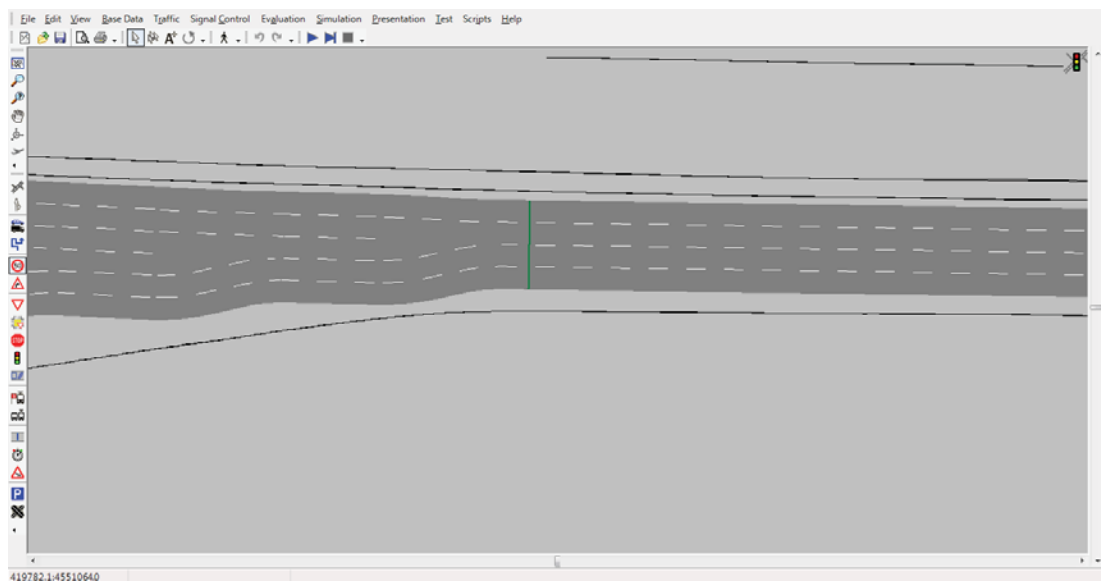


**Figure 5.21:** Desired Speed Decision Locations at the End of Network.

A piecewise function policy is applied and coded in VAP for variable speed limit (VSL) approach in this study. This may be shown as

$$u'(t + \Delta t) = \begin{cases} u_1 & , o(t + \Delta t) < o_1 \\ u_2 & , o_1 \leq o(t + \Delta t) < o_2 \\ u_3 & , o_2 \leq o(t + \Delta t) < o_3 \\ u_4 & , o_3 \leq o(t + \Delta t) < o_4 \\ u_5 & , o_4 \leq o(t + \Delta t) \end{cases} \quad (5.4)$$

where  $u'(t + \Delta t)$  is the shown desired speed for the related vehicle type in the next cycle time. In this study, 4 VSL proposal cases are offered which are summarized in Table 5.2.



**Table 5.2:** VSL Cases Offered.

VSL Name	Initial Case				$o_1$	$o_2$	$o_3$	$o_4$	$o(t + \Delta t) < o_1$				$o_1 \leq o(t + \Delta t) < o_2$				$o_2 \leq o(t + \Delta t) < o_3$			
	Main Stream		Ramp						Main Stream		Ramp		Main Stream		Ramp		Main Stream		Ramp	
	Cars	HGV	Cars	HGV					Cars	HGV	Cars	HGV	Cars	HGV	Cars	HGV	Cars	HGV	Cars	HGV
Case 1	90	60	No Control		90	70	No Control		80	70	No Control		70	60	No Control					
Case 2	90	60	80	50	90	70	80	60	80	70	80	60	70	70	70	70	60	60		
Case 3	90	60	80	50	90	90	80	80	80	80	80	80	80	70	70	70	70	70		
Case 4	90	60	80	50	90	90	80	80	80	80	80	80	80	70	70	70	70	70		
VSL Name	$o_3 \leq o(t + \Delta t) < o_4$				$o_4 \leq o(t + \Delta t)$															
	Main Stream		Ramp		Main Stream		Ramp		Main Stream		Ramp		Main Stream		Ramp		Main Stream		Ramp	
	Cars	HGV	Cars	HGV	Cars	HGV	Cars	HGV	Cars	HGV	Cars	HGV	Cars	HGV	Cars	HGV	Cars	HGV	Cars	HGV
Case 1	60	50	No Control		50	50	No Control		50	50	No Control		50	50	No Control					
Case 2	60	60	60	60	50	50	50	50												
Case 3	60	60	60	60	50	50	50	50												
Case 4	60	60	60	60	50	50	50	50												

As it is demonstrated in ramp metering approaches the speed limit fluctuations for every case is demonstrated in Figure 5.22 to 5.26.

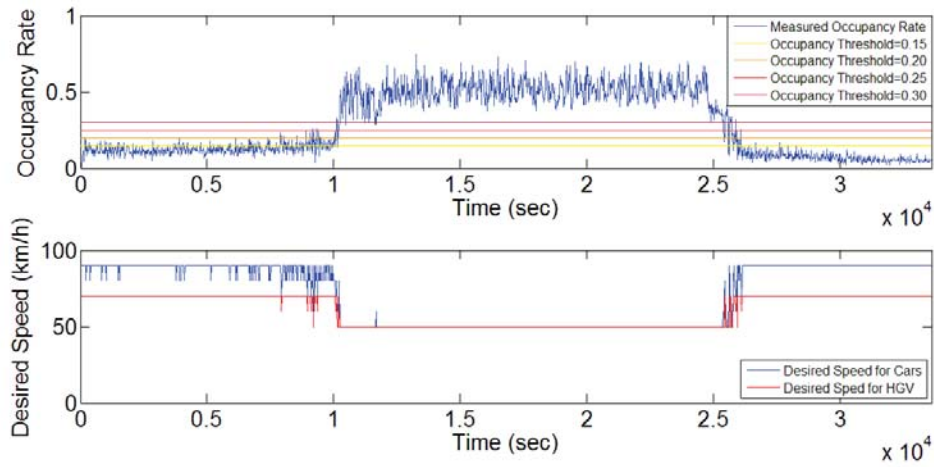


**Figure 5.22:** Desired Speed Fluctuations for VSL Case 1

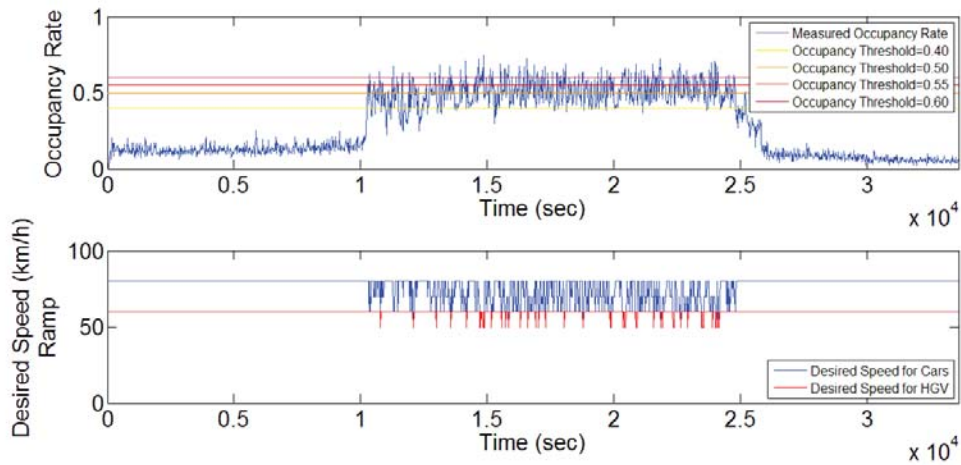


**Figure 5.23:** Desired Speed Fluctuations for VSL Case 2 at the Ramp

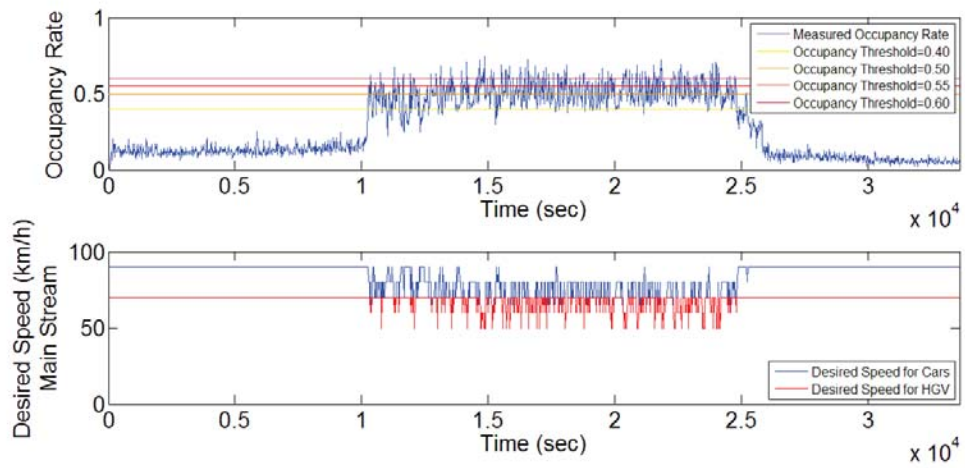


**Figure 5.24:** Desired Speed Fluctuations for VSL Case 2 at the Main Stream

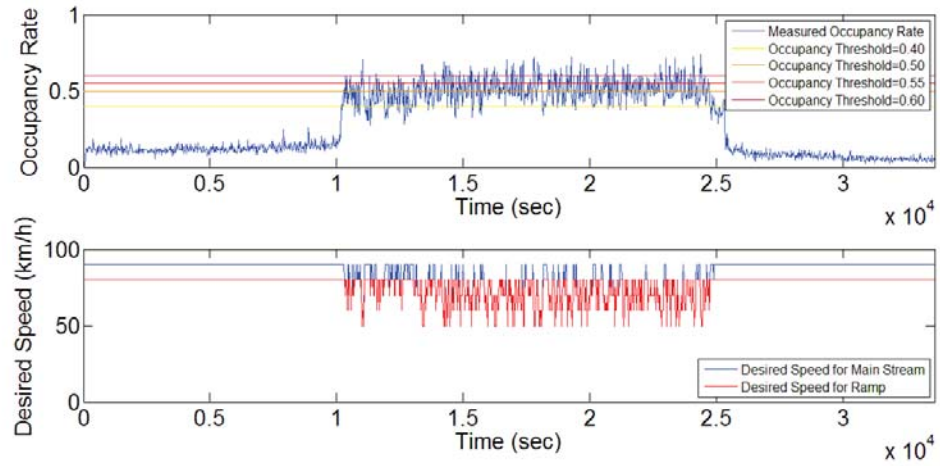


**Figure 5.25:** Desired Speed Fluctuations for VSL Case 3

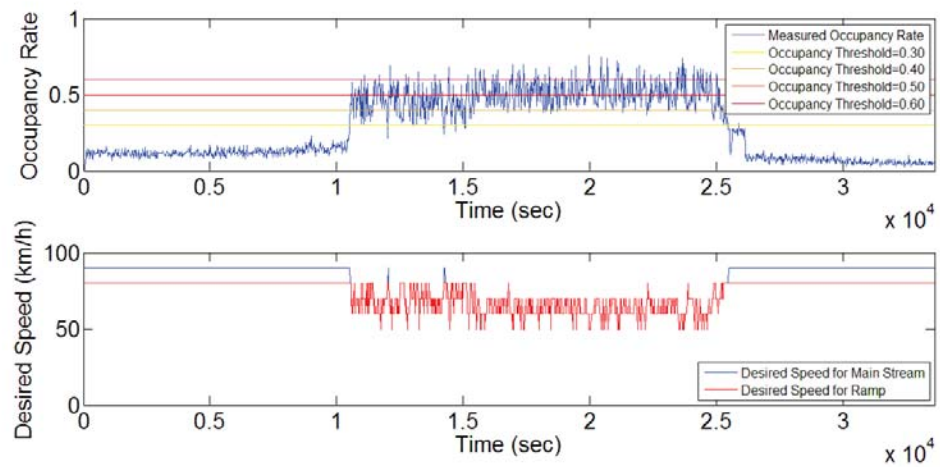


**Figure 5.26:** Desired Speed Fluctuations for VSL Case 4

The density profiles with regard to the VSL Cases are shown in Figure 5.27 to 5.30.

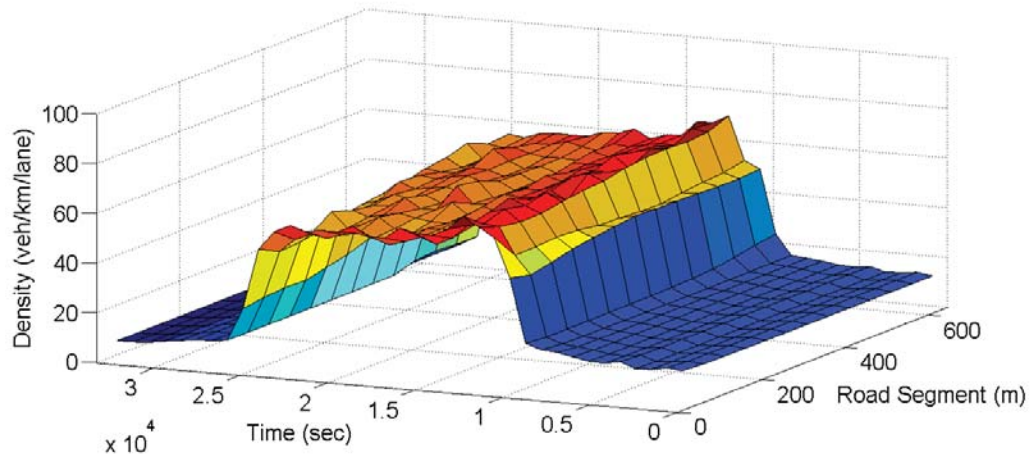


**Figure 5.27:** Density Profile for VSL Case 1.

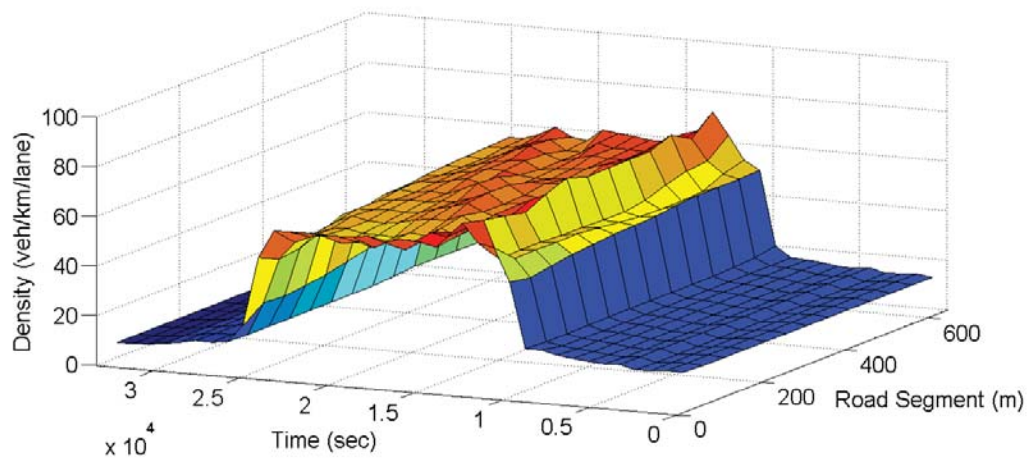


**Figure 5.28:** Density Profile for VSL Case 2.

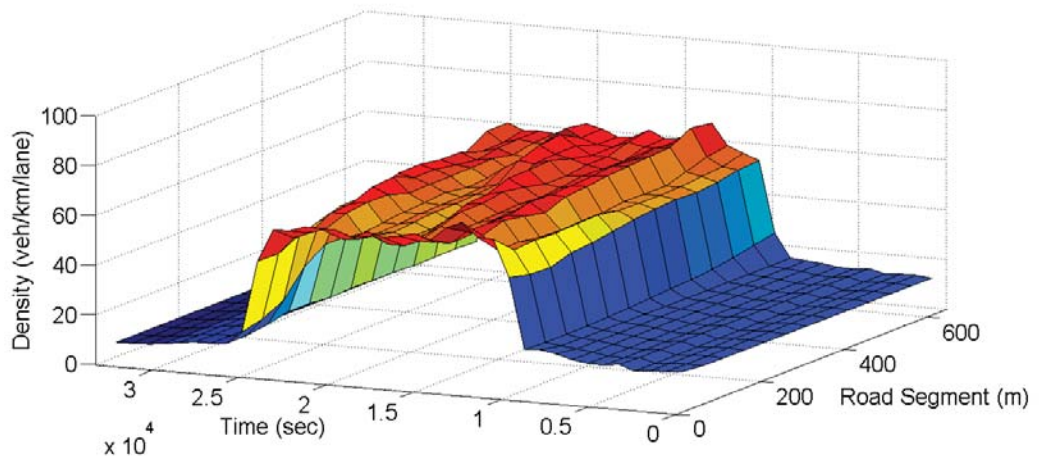


**Figure 5.29:** Density Profile for VSL Case 3.

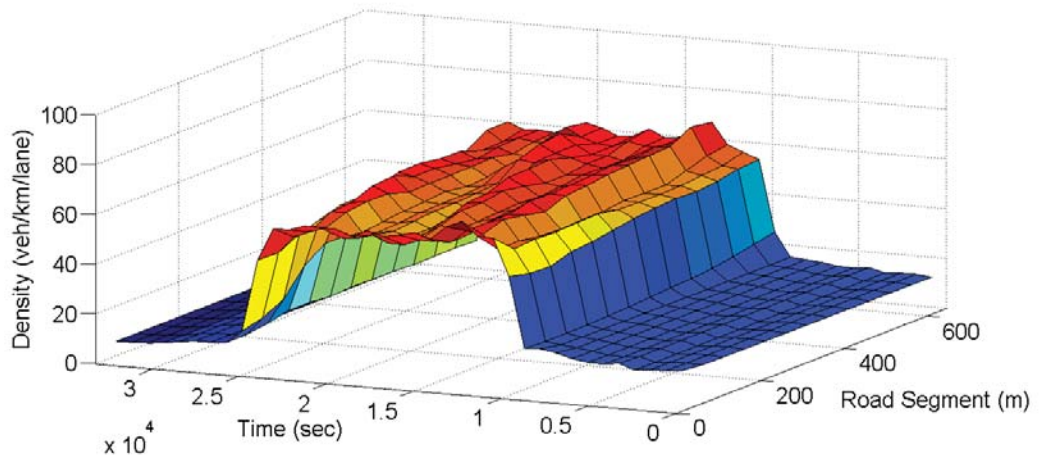


**Figure 5.30:** Density Profile for VSL Case 4.

It is obvious that ramp metering approaches are more suitable than VSL approaches for smoothing the density profile. However, the improvements are little but seen anyway. As it can be seen that Case 2 is the best case for smoothing the density profile.



## 6. CONCLUSION

Two main dynamic traffic flow control approaches are proposed for the traffic congestion at Istanbul Outer Beltway (O-2) in this study. First one is dynamic ramp metering approach, which reduces the traffic congestion at the downstream. The second one is VSL approach.

For each approach, which are dynamic ramp metering case and variable speed limit case, and no control case, simulations are run multiple times in order to check for the consistency of the random seeds which is also proposed in PTV VISSIM Manual [12]. All the multirun performance results are given as Appendix A.

For the simulation performance measures average delay time per vehicle, average number of stops, average speed, average stopped delay per vehicle, total delay time, number of stops, total stopped delay and total travel time are selected.

For the ramp metering approaches ALINEA control algorithm is used. The first ramp metering approach, whose cycle time is 20 seconds and minimum green time is 10 seconds, decreased

- average delay time per vehicle by 32 %,
- average number of stops by 21 %,
- average stopped delay per vehicle by 34 %,
- total delay time by 32 %,
- number of stops by 21 %,
- total stopped delay by 34 % and
- total travel time by 20 %.

This approach also increased average speed of vehicles by 24 %.



The second ramp metering approach, whose cycle time is 15 seconds and minimum green time is 5 seconds, decreased

- average delay time per vehicle by 29 %,
- average number of stops by 21 %,
- average stopped delay per vehicle by 35 %,
- total delay time by 30 %,
- number of stops by 22 %,
- total stopped delay by 35 % and
- total travel time by 18 %.

This approach also increased the average speed of vehicles by 21 %.

For the VSL approaches, various strategies in form of a piecewise function of the detector occupancy rates are offered. In the first approach, there is no control applied on the ramp while a control is applied on the main stream and low rates of occupancy thresholds 0.15, 0.2, 0.25 and 0.3 are tested. In the other approaches a control on the ramp is also applied and the occupancy rate boundaries of the piecewise function are raised in the second approach to 0.4, 0.5, 0.55, 0.6; in the third approach to 0.45, 0.5, 0.55, 0.6 and in the fourth approach to 0.3, 0.4, 0.5, 0.6. In the both first two approaches desired speed decisions are assigned for cars and HGV separately, while in the last two approaches desired speed decisions are assigned for both of the vehicle types. VSL approaches improvements or worsenings do vary in each approach.

The first variable speed limit approach

- decreased average delay time per vehicle by 7 %,
- increased average number of stops by 1 %,
- decreased average speed of vehicles by 3 %,
- decreased average stopped delay per vehicle by 6 %,



- decreased total delay time by 8 %,
- decreased number of stops by 0.3 %,
- decreased total stopped delay by 7 % and
- increased total travel time by 2 %.

The second variable speed limit approach

- decreased average delay time per vehicle by 4 %,
- decreased average number of stops by 2 %,
- decreased average speed of vehicles by 2 %,
- decreased average stopped delay per vehicle by 2 %,
- decreased total delay time by 4 %,
- decreased number of stops by 2 %,
- decreased total stopped delay by 2 % and
- increased total travel time by 1 %.

The third variable speed limit approach

- decreased average delay time per vehicle by 6 %,
- decreased average number of stops by 5 %,
- increased average speed of vehicles by 0.5 %,
- decreased average stopped delay per vehicle by 7 %,
- decreased total delay time by 6 %,
- decreased number of stops by 5 %,
- decreased total stopped delay by 6 % and

- decreased total travel time by 0.6 %.

The fourth variable speed limit approach

- decreased average delay time per vehicle by 10 %,
- decreased average number of stops by 8 %,
- increased average speed of vehicles by 1 %,
- decreased average stopped delay per vehicle by 10 %,
- decreased total delay time by 10 %,
- decreased number of stops by 8 %,
- decreased total stopped delay by 10 % and
- decreased total travel time by 1 %.

The best results are obtained for total travel time in the ramp metering approach whose cycle time is equal to 15 sec and minimum green time to 5 sec. On the other hand, although VSL approaches generally do not have forceful effect on total travel time, they improve other indexes such as average delay time per vehicle or number of stops which reduces the harmful emissions. In the framework of sustainable solutions this is very crucial.

As a future work, coordinative dynamic ramp metering approaches may be done in order to optimize a larger network. Improving traffic flow at one highway section may not be sufficient for a relaxation in a larger network. It may also be harmful to the other consecutive section. That is why, the whole network of Istanbul Outer Beltway (O-2) may be under consideration while optimizing the traffic flow. Dynamic lane closure or openings may also be tested. Ramp Metering and VSL approaches may also be applied in coordination.

In this study, control is made in macroscale. However it is possible to state that, by communicating with the car via radio or car devices may be done in order to have

a control in microscale. Desired speed assignments or dynamic assignments may be done through that way, which will reduce the traffic congestion more.



## REFERENCES

- [1] **Wang, H., Li, J. and Ni, D.**, 2010. Representing the Fundamental Diagram: the Pursuit of Mathematical Elegance and Empirical Accuracy, 89<sup>th</sup> Annual Meeting Transportation Research Board, Washington, D. C., USA.
- [2] [http://en.wikipedia.org/wiki/Traffic\\_flow](http://en.wikipedia.org/wiki/Traffic_flow), accessed at 11.03.2013.
- [3] **Kühne, R.D.**, 2008. Greenshields' Legacy: Highway Traffic, Greenshields Symposium, Massachusetts, USA.
- [4] **Akbas, A. and Ergun, M.**, 2005. Freeway Traffic Flow Control by Lumped Parameter System Approach, *Indian Journal of Engineering & Materials Sciences*, **13 August 2006**, 322–332.
- [5] **Göksu, G., Kesten, A.S., Adanah, P., Ergün, M. and Yai, T.**, 2013. An Analysis on Properties of Lane Based Macroscopic Fundamental Diagram for Urban Highway, 13<sup>th</sup> World Congress on Transportation Research, Rio de Janeiro, Brasil.
- [6] **Mazaré, P.E., Claudel, C.G. and Bayen, A.M.** Analytical and Grid-free Solutions to the Lighthill-Whitham-Richards Traffic Flow Model, *Preprint submitted to Transportation Research*.
- [7] **Daganzo, C.F.**, 1997. Fundamentals of Transportation and Traffic Operations, Pergamon, Great Yarmouth, UK.
- [8] <http://www.isbak.com.tr/Akilli-Ulasim-Sistemleri/Galeri/Degisken-Trafik-Isareti-DTI.html>, accessed at 25.03.2013.
- [9] <http://www.sondakika.com/haber-fatih-sultan-mehmet-koprusu-nde-uc-serit-uc-ay-3714379/>, accessed at 26.06.2013.
- [10] **Burghout, W.**, 2007, Advance Transport Modelling Course Lecture Notes.
- [11] **PTV America Inc.**, 2011, VISSIM Overview Presentation.
- [12] **PTV AG**, 2011, VISSIM 5.40 User Manual.
- [13] **Chowdhury, A.M. and Sadek, A.**, 2003. Fundamentals of Intelligent Transportation Systems Planning, Artech House, Norwood, UK.
- [14] **Sussman, J.M.**, 2005. Perspective on Intelligent Transportation Systems, Springer Verlag, New York, USA.

- [15] **Aksoy, G.**, 2012, Bağ Yolculuk Sürelerinin Ölçüm ve Modelleme Kapsamında İrdelenmesi, MSc. Dissertation, ITU Institute of Science, Transportation Engineering Graduate Program, Istanbul, Turkey.
- [16] **Kesten, A.S.**, 2013, Non-Submitted PhD. Dissertation Draft, ITU Institute of Science, Transportation Engineering Graduate Program, Istanbul, Turkey.
- [17] **Ulucay, S.**, 2011. Traffic Management in an Intercontinental City: Istanbul, 1<sup>st</sup> International Conference on Access Management, Athens, Greece.
- [18] **Akbas, A. and Ergun, M.**, 2005. Dynamic Traffic Signal Control Using a Nonlinear Coupled Oscillators Approach, *Canadian Journal of Civil Engineering*, **32**, 430–441.
- [19] **Papageorgiou, M., Hadj-Salem, H. and Blosseville, J.M.**, 1991. ALINEA: A Local Feedback Control Law for On-Ramp Metering, *Transportation Research Record 1320*, 58–64.
- [20] **Lighthill, M.J. and Whitham, G.B.**, 1955. On Kinematic Waves. II. A Theory of Traffic Flow on Long Crowded Roads, *Proceedings of the Royal Society A*, **229**, 317–345.
- [21] **Richards, P.I.**, 1956. Shock Waves on the Highway, *Operations Research*, **4**, 42–51.
- [22] **Daganzo, C.F.**, 1994. The Cell Transmission Model: A Dynamic Representation of Highway Traffic Consistent with the Hydrodynamic Theory, *Transportation Research Part B: Methodological*, **28(4)**, 269–287.
- [23] **Godunov, S.K.**, 1959. A Difference Method for Numerical Calculation of Discontinuous Solutions of the Equations of Hydrodynamics, *Matematicheskii Sbornik*, **47(3)**, 271–306.
- [24] **Whitham, G.B.**, 1997. Linear and Nonlinear Waves, John Wiley & Sons Inc., USA.
- [25] <http://www.fhwa.dot.gov/publications/research/operations/tft/index.cfm>, accessed at 11.03.2013.
- [26] **HCM**, 2010. Highway Capacity Manual, *Transportation Research Board*.
- [27] **Wardrop, J.G.**, 1952. Some Theoretical Aspects of Road Traffic Research, Proceedings of the Institution of Civil Engineers, Part II, volume I, pp.325–362.
- [28] **Greenshields, B.**, 1935. A Study of Traffic Capacity, Proceedings of the Highway Research Board, volume 14, pp.448–477.
- [29] **Payne, H.J.**, 1971. Models of Freeway Traffic and Control, Simulation Council Proceedings in Series Mathematical Models of Public Systems, La Jolia, California, USA, pp.51–61.

- [30] **Daganzo, C.F.**, 1995. Requiem for High-Order Fluid Approximations of Traffic Flow, *Transportation Research Part B: Methodological*, **29(4)**, 277–287.
- [31] **Aw, A. and Rascle, M.**, 2000. Resurrection of "Second Order" Models of Traffic Flow, *SIAM Journal of Applied Mathematics*, **60**, 916–938.
- [32] **Colombo, R.M.**, 2002. A 2x2 Hyperbolic Traffic Flow Model, *Mathematical and Computer Modelling*, **35(5-6)**, 683–688.
- [33] **Goatin, P.**, 2009, Analyse et Approximation Numérique de Quelques Modèles Macroscopiques de Trafic Routier, HDR (Habilitation a Diriger der Recherches).
- [34] **Goatin, P.**, 2006. The Aw-Rascle Traffic Flow Model with Phase Transitions, *Mathematical and Computer Modelling*, **44**, 287–303.
- [35] **Goatin, P.**, 2011. The Aw-Rascle Traffic Model with Locally Constrained Flow, *Journal of Mathematical Analysis and Applications*, **378(2)**, 634–648.
- [36] **Papageorgiou, M., Diakaki, C., Dinopoulou, V., Kotsialos, A. and Wang, Y.**, 2003. Review of Road Traffic Control Strategies, *Proceedings of the IEEE*, **91(12)**, 2043–2067.
- [37] **Hegyi, A., De Schutter, B. and Hellendoorn, H.**, 2005. Model predictive control for optimal coordination of ramp metering and variable speed limits, *Transportation Research Part C: Emerging Technologies*, **13(3)**, 185–209.
- [38] **Chaudhary, N.A., Tian, Z., Messer, C.J. and Chu, C.L.**, 2004. Ramp Metering Algorithms and Approaches for Texas, *Texas Transportation Institute Technical Report*.
- [39] **Kachroo, P. and Özbay, K.**, 2003. Feedback Ramp Metering Intelligent Transportation Systems, Springer.
- [40] **Taylor, C., Meldrum, D. and McCormick, D.** Evaluation of a Fuzzy Logic Ramp Metering Algorithm.
- [41] **Jacobson, L.N., Henry, K.C. and Mehyar, O.**, 1989. Real-time metering algorithm for centralized control, 1232.
- [42] **Lau, R.**, 1997. Ramp metering by zone—The Minnesota algorithm, *Minnesota Dept. of Transportation. USA*.
- [43] **Xin, W., Michalopoulos, P.G., Hourdakis, J. and Lau, D.**, 2004. Minnesota's new ramp control strategy: design overview and preliminary assessment, *Transportation Research Record: Journal of the Transportation Research Board*, **1867(1)**, 69–79.
- [44] **Corcoran, L.J. and Hickman, G.A.**, 1989. Freeway ramp metering effects in Denver, Institute of Transportation Engineers Meeting.

- [45] **Papageorgiou, M., Hadj-Salem, H. and Middelham, F.**, 1997. ALINEA local ramp metering: Summary of field results, *Transportation Research Record: Journal of the Transportation Research Board*, **1603(1)**, 90–98.
- [46] **Paesani, G., Kerr, J., Perovich, P. and Khosravi, F.**, 1997. System wide adaptive ramp metering (SWARM), Merging the Transportation and Communications Revolutions. Abstracts for ITS America Seventh Annual Meeting and Exposition.
- [47] **Kang, K.P., Chang, G.L. and Zou, N.**, 2004. Optimal dynamic speed-limit control for highway work zone operations, *Transportation Research Record: Journal of the Transportation Research Board*, **1877(1)**, 77–84.
- [48] **Pal, R. and Sinha, K.C.**, 1996. Evaluation of crossover and partial lane closure strategies for interstate work zones in Indiana, *Transportation Research Record: Journal of the Transportation Research Board*, **1529(1)**, 10–18.
- [49] **Dym, C.**, 2004. Principles of Mathematical Modeling, Elsevier Academic Press, USA.
- [50] **Wiedemann, R.**, 1974. Simulation des Straßenverkehrsflusses, *Schriftenreihe des Instituts für Verkehrswesen der Universität Karlsruhe*, **Heft 8**.
- [51] **Wiedemann, R.**, 1991. Modeling of RTI-Elements on multi-lane Roads, Advanced Telematics in Road Transport, European Community, DG XIII, Brussels, Belgium.
- [52] **Fellendorf, M. and Vortisch, P.**, 2010. Microscopic traffic flow simulator VISSIM. Fundamentals of Traffic Simulation, Springer Verlag, New York, USA, pp.63–93.
- [53] **Chu, L., Liu, H.X., Oh, J.S. and Recker, W.**, 2004. A Calibration procedure for Microscopic Traffic Simulation, 83<sup>rd</sup> Annual Meeting Transportation Research Board, Washington, D. C., USA.
- [54] **Gao, Y.**, 2008, Calibration and Comparison of the VISSIM and INTEGRATION Microscopic Traffic Simulation Models, MSc. Dissertation, Faculty of the Virginia Polytechnic Institute and State University, Civil and Environmental Engineering Graduate Program, Blacksburg, Virginia, USA.
- [55] **Chu, L. and Yang, X.**, 2003. Optimization of the ALINEA Ramp-metering Control Using Genetic Algorithm with Micro-simulation, 82<sup>nd</sup> Annual Meeting Transportation Research Board, Washington, D. C., USA.
- [56] <http://www.ce.berkeley.edu/~daganzo/Simulations/MFD/MFD.html>, accessed at 02.03.2013.
- [57] **Geroliminis, N. and Daganzo, C.F.**, 2007. Macroscopic Modeling of Traffic in Cities, 86<sup>th</sup> Annual Meeting Transportation Research Board, Washington, D. C., USA.



- [58] **Haberman, R.**, 1998. Mathematical Models: Mechanical Vibrations, Population Dynamics and Traffic Flow, Society for Industrial and Applied Mathematics (SIAM), Philadelphia, USA.



## **APPENDICES**

### **APPENDIX A: Multirun Simulation Network Performance Results**



## APPENDIX A

**Table A.1:** Average Delay Time per Vehicle in seconds.

Random Seed	No Control	ALINEA (CT=15 sec, minGT=5 sec)	ALINEA (CT=20 sec, minGT=10 sec)	VSL Case 1	VSL Case 2	VSL Case 3	VSL Case 4
5	221.975	153.529	163.085	209.565	213.914	217.912	205.613
15	225.02	154.947	167.798	213.389	214.086	215.804	203.884
25	220.198	157.032	155.824	198.173	216.236	212.369	203.873
35	221.868	151.895	157.606	200.112	216.68	204.203	199.805
45	224.031	151.964	164.048	212.517	217.18	204.308	204.93
55	231.823	153.802	169.297	214.556	212.613	208.754	196.862
65	229.001	154.273	154.167	216.703	220.444	211.62	209.076
75	213.454	145.573	153.431	202.616	207.318	210.251	198.704
85	226.659	151.516	153.611	205.72	218.125	209.56	207.423
95	227.827	151.843	153.259	202.871	218.439	204.645	189.88
Mean	224.186	152.637	159.213	207.622	215.504	209.943	202.005
Std. Dev.	5.196	3.023	6.268	6.57	3.72	4.726	5.746

**Table A.2:** Average Number of Stops per Vehicles.

Random Seed	No Control	ALINEA (CT=15 sec, minGT=5 sec)	ALINEA (CT=20 sec, minGT=10 sec)	VSL Case 1	VSL Case 2	VSL Case 3	VSL Case 4
5	1.35	1.042	1.076	1.314	1.255	1.317	1.246
15	1.3	1.09	1.186	1.433	1.342	1.313	1.289
25	1.337	1.108	1.071	1.338	1.302	1.255	1.205
35	1.353	1.08	1.056	1.333	1.32	1.266	1.255
45	1.403	1.137	1.107	1.422	1.333	1.273	1.215
55	1.34	1.026	1.061	1.314	1.316	1.277	1.207
65	1.43	1.018	1.031	1.467	1.361	1.334	1.267
75	1.284	1.032	1.016	1.342	1.3	1.271	1.26
85	1.384	1.088	1.019	1.328	1.359	1.29	1.292
95	1.312	1.071	0.998	1.287	1.315	1.248	1.188
Mean	1.349	1.069	1.062	1.358	1.32	1.284	1.242
Std. Dev.	0.046	0.039	0.055	0.06	0.031	0.028	0.037

**Table A.3:** Average Speed in km/h.

Random Seed	No Control	ALINEA (CT=15 sec, minGT=5 sec)	ALINEA (CT=20 sec, minGT=10 sec)	VSL Case 1	VSL Case 2	VSL Case 3	VSL Case 4
5	32.839	40.411	39.132	31.584	32.258	32.159	32.526
15	32.593	40.246	38.62	31.341	32.18	32.194	32.616
25	33.019	39.966	40.066	32.521	32.037	32.629	32.736
35	32.885	40.649	39.847	32.404	31.992	33.287	33.003
45	32.693	40.645	39.073	31.392	31.946	33.441	32.647
55	31.988	40.391	38.425	31.137	32.312	32.953	33.439
65	32.263	40.364	40.324	31.016	31.643	32.587	32.143
75	33.667	41.546	40.417	32.142	32.833	32.906	33.197
85	32.433	40.71	40.367	31.969	31.848	32.773	32.341
95	32.333	40.631	40.431	32.166	31.833	33.275	34.093
Mean	32.671	40.556	39.67	31.767	32.088	32.82	32.874
Std. Dev.	0.471	0.416	0.784	0.541	0.333	0.442	0.578

**Table A.4:** Average Stopped Delay per Vehicle in seconds.

Random Seed	No Control	ALINEA (CT=15 sec, minGT=5 sec)	ALINEA (CT=20 sec, minGT=10 sec)	VSL Case 1	VSL Case 2	VSL Case 3	VSL Case 4
5	30.114	20.248	21.742	29.643	27.738	28.162	27.532
15	29.155	22.37	21.816	28.783	30.213	28.653	28.429
25	28.657	21.072	18.019	25.819	28.291	27.067	23.54
35	28.666	17.004	17.669	30.226	30.268	27.885	27.702
45	30.481	15.655	23.034	30.596	30.59	27.192	29.792
55	33.186	20.84	22.483	29.759	29.223	26.882	23.551
65	30.019	19.252	14.888	27.164	28.432	29.65	28.548
75	25.861	17.799	15.856	25.315	27.921	26.088	26.175
85	32.143	22.059	21.29	25.937	30.842	28.993	27.562
95	28.896	19.775	17.23	26.384	28.706	27.264	24.038
Mean	29.718	19.607	19.403	27.963	29.222	27.784	26.687
Std. Dev.	2.023	2.2	2.984	2.044	1.165	1.089	2.253



**Table A.5:** Total Delay Time in h.

Random Seed	No Control	ALINEA (CT=15 sec, minGT=5 sec)	ALINEA (CT=20 sec, minGT=10 sec)	VSL Case 1	VSL Case 2	VSL Case 3	VSL Case 4
5	3626.016	2491.049	2641.891	3391.92	3495.412	3560.08	3359.092
15	3685.452	2529.128	2718.226	3460.525	3499.765	3537.094	3338.881
25	3603.241	2553.431	2533.827	3210.076	3523.678	3477.254	3338.824
35	3633.155	2470.865	2562.898	3240.376	3529.956	3345.012	3266.979
45	3661.23	2469.505	2647.14	3450.562	3543.771	3355.073	3359.426
55	3799.253	2498.208	2736.267	3478.788	3471.324	3411.961	3222.195
65	3749.445	2509.507	2509.274	3517.396	3603.956	3466.518	3432.566
75	3501.602	2369.208	2504.071	3285.701	3390.228	3451.324	3254.102
85	3722.175	2467.148	2493.91	3344.031	3568.579	3435.511	3400.928
95	3729.145	2474.83	2481.479	3294.116	3566.75	3353.625	3115.238
Mean	3671.071	2483.288	2582.898	3367.349	3519.342	3439.345	3308.823
Std. Dev.	85.407	49.083	95.504	107.792	60.085	74.955	94.523

**Table A.6:** Total Distance Traveled in km.

Random Seed	No Control	ALINEA (CT=15 sec, minGT=5 sec)	ALINEA (CT=20 sec, minGT=10 sec)	VSL Case 1	VSL Case 2	VSL Case 3	VSL Case 4
5	198602.816	198234.394	197634.503	197160.238	198547.03	198694.2	198514.12
15	199181.496	199426.955	197977.666	197562.845	198836.04	199297.65	199072.58
25	199034.163	198638.763	198229.204	197305.75	198157.81	199170.44	199202.08
35	199299.119	198739.873	198393.549	196876.949	198072.84	199063.31	198698.3
45	198907.712	198610.638	197193.724	197496.955	198442.93	199849.52	199345.6
55	199120.873	198383.691	197385.376	197360.994	198517.18	198817.26	199174.01
65	199159.624	198807.07	198574.108	197450.376	198746.23	199049.54	199403.19
75	199741.924	198927.843	199141.965	197717.675	198802.49	199764.14	199179.92
85	199588.231	198961.061	197983.89	198013.271	198780.18	199123.15	199261.32
95	198997.314	199039.245	197683.089	197702.33	198546.39	199193.36	199560.39
Mean	199163.327	198776.953	198019.707	197464.738	198544.91	199202.26	199141.15
Std. Dev.	326.541	340.918	586.879	317.357	264.757	365.161	316.395

**Table A.7:** Number of Stops.

Random Seed	No Control	ALINEA (CT=15 sec, minGT=5 sec)	ALINEA (CT=20 sec, minGT=10 sec)	VSL Case 1	VSL Case 2	VSL Case 3	VSL Case 4
5	79380	60884	62729	76571	73831	77478	73275
15	76677	64071	69149	83657	78961	77464	76008
25	78787	64846	62703	78053	76383	73949	71055
35	79771	63231	61835	77680	77414	74677	73884
45	82550	66535	64288	83124	78320	75250	71715
55	79037	59973	61744	76672	77346	75156	71124
65	84313	59606	60395	85721	80118	78646	74875
75	75804	60447	59692	78371	76528	75139	74290
85	81843	63801	59548	77712	80023	76127	76284
95	77298	62814	58189	75209	77274	73623	70185
Mean	79546	62620.8	62027.2	79277	77619.8	75750.9	73269.5
Std. Dev.	2692.068	2309.878	3089.284	3550.973	1874.361	1644.788	2160.789

**Table A.8:** Number of Vehicles in the Network.

Random Seed	No Control	ALINEA (CT=15 sec, minGT=5 sec)	ALINEA (CT=20 sec, minGT=10 sec)	VSL Case 1	VSL Case 2	VSL Case 3	VSL Case 4
5	142	142	142	141	148	145	145
15	135	136	136	133	139	137	137
25	116	116	116	116	118	117	118
35	135	136	136	132	139	137	135
45	124	121	123	121	126	124	122
55	139	136	138	133	138	137	137
65	131	132	132	126	131	131	131
75	134	133	133	130	133	133	136
85	153	153	154	150	154	151	150
95	131	132	132	131	135	134	134
Mean	134	133.7	134.2	131.3	136.1	134.6	134.5
Std. Dev.	9.967	10.209	10.229	9.546	10.268	9.617	9.466

**Table A.9:** Number of Vehicles that have left the Network.

Random Seed	No Control	ALINEA (CT=15 sec, minGT=5 sec)	ALINEA (CT=20 sec, minGT=10 sec)	VSL Case 1	VSL Case 2	VSL Case 3	VSL Case 4
5	58665	58269	58176	58127	58677	58669	58668
15	58827	58625	58182	58248	58712	58868	58818
25	58793	58422	58423	58198	58546	58828	58839
35	58816	58425	58405	58162	58509	58834	58728
45	58709	58381	57968	58331	58616	58994	58893
55	58860	58339	58047	58237	58639	58703	58787
65	58812	58428	58463	58307	58724	58840	58973
75	58922	58457	58621	58249	58737	58962	58820
85	58966	58466	58293	58369	58743	58867	58876
95	58795	58543	58157	58324	58647	58861	58929
Mean	58816.5	58435.5	58273.5	58255.2	58655	58842.6	58833.1
Std. Dev.	88.836	99.562	203.517	78.122	80.277	99.262	91.324

**Table A.10:** Total Stopped Delay in h.

Random Seed	No Control	ALINEA (CT=15 sec, minGT=5 sec)	ALINEA (CT=20 sec, minGT=10 sec)	VSL Case 1	VSL Case 2	VSL Case 3	VSL Case 4
5	491.919	328.537	352.207	479.792	453.247	460.093	449.79
15	477.516	365.13	353.413	466.769	493.913	469.633	465.561
25	468.935	342.643	293.001	418.226	461.02	443.189	385.515
35	469.412	276.596	287.325	489.441	493.098	456.772	452.943
45	498.134	254.4	371.687	496.783	499.152	446.53	488.382
55	543.874	338.503	363.386	482.503	477.128	439.379	385.479
65	491.499	313.172	242.323	440.911	464.821	485.695	468.689
75	424.234	289.686	258.772	410.516	456.58	428.241	428.661
85	527.854	359.191	345.647	421.617	504.582	475.305	451.912
95	472.984	322.3	278.971	428.404	468.727	446.792	394.38
Mean	486.636	319.016	314.673	453.496	477.227	455.163	437.131
Std. Dev.	33.221	35.977	47.544	32.948	19.001	17.752	36.955

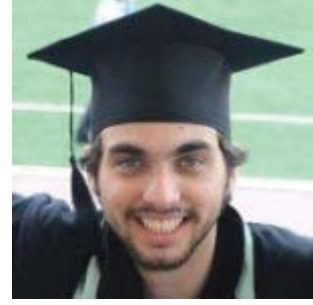
**Table A.11:** Total Travel Time in h.

Random Seed	No Control	ALINEA (CT=15 sec, minGT=5 sec)	ALINEA (CT=20 sec, minGT=10 sec)	VSL Case 1	VSL Case 2	VSL Case 3	VSL Case 4
5	6047.853	4905.439	5050.456	6242.455	6154.983	6178.437	6103.325
15	6111.205	4955.227	5126.365	6303.752	6178.914	6190.44	6103.434
25	6027.825	4970.155	4947.618	6066.938	6185.269	6104.064	6085.055
35	6060.504	4889.165	4978.879	6075.775	6191.398	5980.23	6020.613
45	6084.085	4886.483	5046.851	6291.35	6211.905	5976.231	6106.117
55	6224.842	4911.556	5136.952	6338.435	6143.785	6033.449	5956.416
65	6173.081	4925.356	4924.459	6366.047	6280.983	6108.305	6203.675
75	5932.848	4788.092	4927.208	6151.337	6054.982	6070.682	5999.97
85	6153.823	4887.3	4904.559	6193.893	6241.477	6075.824	6161.351
95	6154.592	4898.729	4889.334	6146.351	6237.213	5986.239	5853.359
Mean	6097.066	4901.75	4993.268	6217.633	6188.091	6070.39	6059.332
Std. Dev.	84.672	49.141	91.021	106.958	62.663	77.551	103.287





## CURRICULUM VITAE



**Name Surname:** Gökhan GÖKSU

**Place and Date of Birth:** Istanbul, 22.12.1988

**Address:** Hamidiye Mah. Osman Gazi Cad. Huzur Sok. Çınar Apt. Daire 9  
34408 Kağıthane Istanbul/TURKEY

**E-Mail:** goksug@itu.edu.tr, goekhan.goeksu@gmail.com

**Web:** <http://web.itu.edu.tr/goksug>, <http://istanbultek.academia.edu/GökhanGöksu>

**B.Sc.:** Major on Mathematical Engineering (2011), ITU

Minor on Physical Engineering (Ongoing), ITU

**Professional Experience and Rewards:** Honor List at graduation.

### List of Publications and Patents:

- **Göksu, G.**, Kesten, A. S., Adanalı, P., Ergün, M. and Yai, T., "An Analysis on Properties of Lane Based Macroscopic Fundamental Diagram for Urban Highway", *World Conference on Transportation Research*, Rio, 15.07.2013 - 18.07.2013.

### PUBLICATIONS/PRESENTATIONS ON THE THESIS

- **Göksu, G.**, Kesten, A. S., Ergün, M. and Akbaş, A., "A Dynamic Speed Limit Control Approach for Highway Bottleneck Management", *1<sup>st</sup> International Symposium on Innovative Technologies in Engineering and Science*, Sakarya, 07.06.2013-09.06.2013.